

I-Con: A UNIFYING FRAMEWORK FOR REPRESENTATION LEARNING

000
001
002
003
004
005
006
007
008
009
010
011
012
013
014
015
016
017
018
019
020
021
022
023
024
025
026
027
028
029
030
031
032
033
034
035
036
037
038
039
040
041
042
043
044
045
046
047
048
049
050
051
052
053
Anonymous authors
Paper under double-blind review

ABSTRACT

As the field of unsupervised learning grows, there has been a proliferation of different loss functions to solve different classes of problems. We find that a large collection of modern loss functions can be generalized by a single equation rooted in information theory. In particular, we introduce I-Con, a framework that shows that several broad classes of machine learning methods are precisely minimizing an integrated KL divergence between two conditional distributions: the supervisory and learned representations. This viewpoint exposes a hidden information geometry underlying clustering, spectral methods, dimensionality reduction, contrastive learning, and supervised learning. I-Con enables the development of new loss functions by combining successful techniques from across the literature. We not only present a wide array of proofs, connecting over 11 different approaches, but we also leverage these theoretical results to create state of the art unsupervised image classifiers that achieve a +8% improvement over the prior state-of-the-art on unsupervised classification on ImageNet-1K.

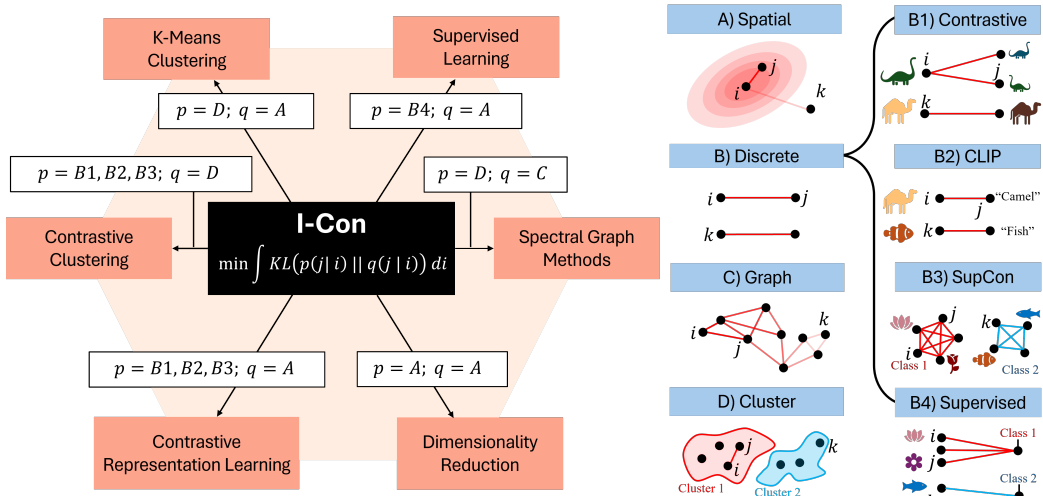


Figure 1: **I-Con unifies representation learning methods.** By choosing different types of conditional probability distributions over neighbors, I-Con generalizes over 11 commonly used representation learning methods.

1 INTRODUCTION

In the past 10 years the field of representation learning has flourished, with new techniques, architectures, and loss functions emerging daily. These advances have powered humanities’ most intelligent models and have enabled machines to rely less and less on human supervision. However, as the field of unsupervised learning grows, the number of distinct and specific loss functions grows in turn making it difficult to understand which particular loss function to choose for a given problem or domain. In this work we propose a novel mathematical framework that unifies several broad classes

of supervised and unsupervised representation learning systems with a single information-theoretic equation. Our framework, which we call Information Contrastive learning (I-Con) demonstrates that many methods in clustering, spectral graph theory, contrastive learning, dimensionality reduction, and supervised learning are all specific instances of the same underlying loss function. Though some specific connections implied by I-Con have been documented or approximated in the literature Balestrier & LeCun (2022); Yang et al. (2022); Böhm et al. (2022); Hu et al. (2022), to the best of the authors knowledge this is the first time the theory has been described in general. I-Con not only unifies a broad swath of literature but provides a framework to build and discover new loss functions and learning paradigms. In particular, the framework allows us to move techniques and results from any given method, to improve every other method in the broader class. We use this technique to derive new loss functions for unsupervised image classification that significantly outperform the prior art on several standard datasets. We summarize our contributions:

- We present I-Con, a single equation that unifies several broad classes of methods in representation learning
- We prove 9 theorems which connect a variety of methods to the I-Con framework
- We use I-Con to derive new improvements for unsupervised image classification and achieve a +8% increase in unsupervised ImageNet-1K accuracy over the prior state-of-the-art
- We carefully ablate our discovered improvements, demonstrating their efficacy.

2 RELATED WORK

Representation learning is a vast field with thousands of methods, we overview some of the key methods that I-Con leverages and generalizes. We refer the interested reader to Le-Khac et al. (2020); Bengio et al. (2013); Weng (2021) for more complete reviews of the representation and contrastive learning literature.

Feature Learning aims to learn informative low-dimensional continuous vectors from high dimensional data. Feature learners come in a variety of flavors, using supervisory signals like distance in a high dimensional space, nearest neighbors, known positive and negative pairs, auxiliary supervised losses, and reconstruction loss. The most common methods learn directly from distances between points in high dimensional space such as PCA Pearson (1901) which optimizes for reconstruction error, MDS Kruskal (1964) which preserves distances between points. Other approaches try to match pairwise high-dimensional distances, neighborhoods, or topological structure with low dimensional vectors. Techniques include UMAP McInnes et al. (2018) which preserves a soft topology of the points, and SNE/t-SNE Hinton & Roweis (2002); Van der Maaten & Hinton (2008) that use a KL divergence to align joint distributions across low and high dimensional views of the data. SNE and t-SNE were some of the first works to explicitly phrase their optimization in terms of KL minimization between two joint distributions, which is the central idea of I-Con. Methods like SimCLR Chen et al. (2020a), CMC Tian et al. (2020), CLIP Radford et al. (2021), MoCo v3 Chen* et al. (2021), and others use positive and negative pairs of data, often formed through augmentations or aligned corpora to drive feature learning. I-Con generalizes all of these frameworks and through our analysis the subtle differences in how they implicitly construct their losses becomes apparent. Finally, one of the most famous approaches for representation learning in fields like computer vision, uses the penultimate activations of a supervised classifier as informative features Krizhevsky et al. (2017). Interestingly, I-Con generalizes this case as well if we consider discrete class labels as “points” in a contrastive learning setup. This provides an intuitive justification for why penultimate activations of supervised activations make high quality representations.

Clustering aims to learn a discrete representation for data, again using distances in ambient space, nearest neighbors, or contrastive supervision. Classic methods like k-Means Macqueen (1967) and EM Dempster et al. (1977) implicitly fit cluster distributions to data points to maximize data likelihood. Spectral Clustering Shi & Malik (2000) uses the spectra of the graph Laplacian to cut a graph into two strongly connected components. Methods like IIC Ji et al. (2019) and Contrastive Clustering Li et al. (2021) use augmentation invariance to drive learning. SCAN Gansbeke et al. (2020) realized that including nearest neighbors as contrastive positive pairs could improve clustering and

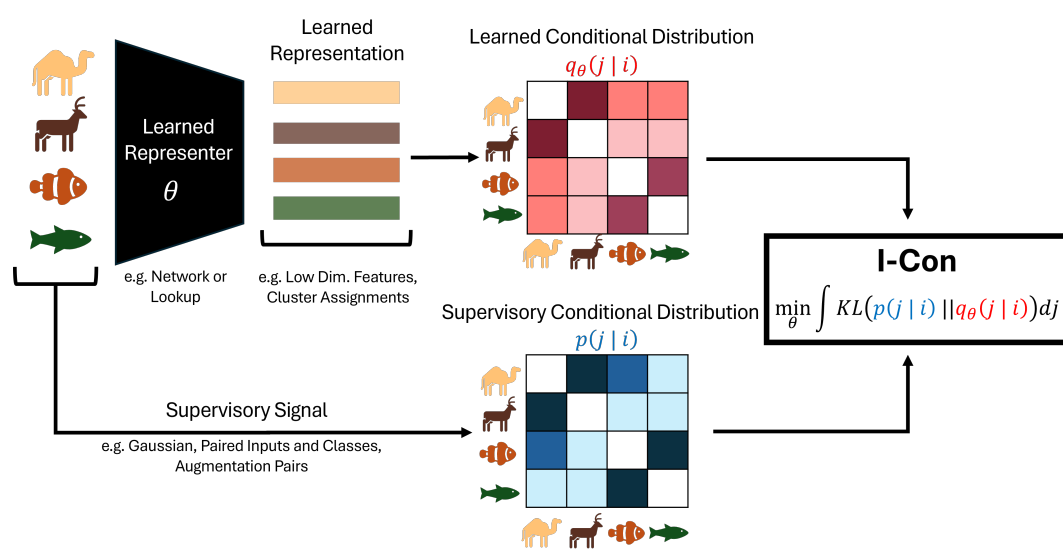


Figure 2: Architecture diagram of an I-Con model. I-Con aligns a parameterized neighborhood distribution computed from a learned representation, with a supervisory neighborhood distribution chosen by the method designer.

most recently TEMI Adaloglou et al. (2023) shows that student-teacher style EMA architectures Chen et al. (2020b) can also improve outcomes. I-Con generalizes many of these methods, by aligning a cluster-induced joint distribution with a supervisory joint distribution derived from either distances, the graph Laplacian, or contrastive pairs. Improvements like EMA-style architectures can be included naturally in I-Con as different parameterizations of the clusters that are optimized with the central I-Con loss.

Unifying unsupervised learning methods has been a goal of several existing and seminal works in the literature. Hu et al. (2022) discovered that contrastive learning and t-SNE could be seen as two different aspects of the same loss. Yang et al. (2022) found that cross-entropy and contrastive learning could be unified by considering different kinds of neighbor relations between points. Balestrierio & LeCun (2022) found approximate connections between spectral methods and contrastive learning. Grosse et al. (2012) showed how many common classical unsupervised learners can be derived with Bayesian tensor factorization grammars. Tschannen et al. (2019) critically examined mutual information maximization for representation learning, highlighting the role of architectural choices and estimator parameterizations in addition to the MI maximization itself, though their analysis does not attempt a broader unification across diverse methods. These prior works are elegant and impactful; however, to the best of our knowledge, we are the first to describe the unification of supervised, contrastive, dimensionality reduction, spectral graph, and clustering methods using a single KL divergence loss.

3 METHODS

The I-Con framework unifies several representation learning methods using a single loss function: minimizing the KL divergence between a pair of conditional “neighborhood distributions” which measure the probability of transition from a data point i to a point j . I-Con’s single information-theoretic objective generalizes methods from the fields of clustering, contrastive learning, dimensionality reduction, spectral graph theory, and supervised learning. By choosing how we construct the supervisory neighborhood distribution, and parameterize the neighborhood distribution of the learned representation, we can create a broad class of existing and novel methods using I-Con. We first introduce I-Con, then use the framework to aggregate important techniques from across the broader literature to make a novel state of the art unsupervised image classification method.

162

163

164

165

166

167

168

169

170

171

172

173

174

175

176

177

178

179

180

181

182

183

184

185

186

187

188

189

190

191

192

193

194

195

196

197

198

199

200

201

202

203

204

205

206

207

208

209

210

211

212

213

214

215

Method	Choice of $p_\theta(j i)$	Choice of $q_\phi(j i)$
SNE Hinton & Roweis (2002) Theorem 1	Gaussians on datapoints, x_i $\frac{\exp(-\ x_i - x_j\ ^2/2\sigma_i^2)}{\sum_{k \neq i} \exp(-\ x_i - x_k\ ^2/2\sigma_i^2)}$	Gaussians on learned vectors, ϕ_i $\frac{\exp(-\ \phi_i - \phi_j\ ^2)}{\sum_{k \neq i} \exp(-\ \phi_i - \phi_k\ ^2)}$
tSNE Van der Maaten & Hinton (2008) Theorem 2	Perplexity-sized Gaussians on datapoints, x_i $\frac{\exp(-\ x_i - x_j\ ^2/2\sigma_i^2)}{\sum_{k \neq i} \exp(-\ x_i - x_k\ ^2/2\sigma_i^2)}$	Cauchy distributions on learned vectors, ϕ_i $\frac{(1 + \ \phi_i - \phi_j\ ^2)^{-1}}{\sum_{k \neq i} (1 + \ f\phi_i - \phi_k\ ^2)^{-1}}$
InfoNCE Bachman et al. (2019) Theorem 4	Uniform over positive pairs $\frac{1}{Z} \mathbb{1}[i \text{ and } j \text{ are positive pairs}]$	Gaussian based on deep features, $f_\phi(x_i)$ $\frac{\exp(-\ f_\phi(x_i) - f_\phi(x_j)\ ^2)}{\sum_{k \neq i} \exp(-\ f_\phi(x_i) - f_\phi(x_k)\ ^2)}$
Triplet Loss Schroff et al. (2015) Theorem 5	Uniform over positive pairs $\frac{1}{Z} \mathbb{1}[i \text{ and } j \text{ are positive pairs}]$	Gaussian based on deep features $f_\phi(x_i)$, with only one negative sample and $\sigma \rightarrow 0$ $\frac{\exp(-\ f_\phi(x_i) - f_\phi(x_j)\ ^2/2\sigma^2)}{\sum_{k \in \{i^+, i^-\}} \exp(-\ f_\phi(x_i) - f_\phi(x_k)\ ^2/2\sigma^2)}$
PCA Pearson (1901) Corollary 1	Indicator over the point itself $\mathbb{1}[i = j]$	Wide Gaussian on features based on a linear map $f_\phi(x_i)$ for x_i $\lim_{\sigma \rightarrow \infty} \frac{\exp(-\ \phi_i - \phi_j\ ^2/2\sigma^2)}{\sum_{k \neq i} \exp(-\ \phi_i - \phi_k\ ^2/2\sigma^2)}$
MDS Kruskal (1964) Theorem 3	Wide Gauss. on datapoints, x_i $\lim_{\sigma \rightarrow \infty} \frac{\exp(-\ x_i - x_j\ ^2/2\sigma_i^2)}{\sum_{k \neq i} \exp(-\ x_i - x_k\ ^2/2\sigma_i^2)}$	Wide Gauss. on learned vectors., $\phi_i f_\phi(x_i)$ $\lim_{\sigma \rightarrow \infty} \frac{\exp(-\ \phi_i - \phi_j\ ^2/2\sigma^2)}{\sum_{k \neq i} \exp(-\ \phi_i - \phi_k\ ^2/2\sigma^2)}$
InfoNCE Clustering (New in this work)	Uniform over positive pairs $\frac{1}{Z} \mathbb{1}[i \text{ and } j \text{ are positive pairs}]$	Shared cluster likelihood by point $\frac{f_\phi(x_i) \cdot f_\phi(x_j)}{\mathbb{E}[\text{size of } x_i \text{'s cluster w.r.t } f_\phi]}$
SupCon Khosla et al. (2020) Theorem 2	Uniform over classes $\frac{1}{Z} \mathbb{1}[i \text{ and } j \text{ have the same class}]$	Gaussian based on deep features, $f_\phi(x_i)$ $\frac{\exp(-\ f_\phi(x_i) - f_\phi(x_j)\ ^2)}{\sum_{k \neq i} \exp(-\ f_\phi(x_i) - f_\phi(x_k)\ ^2)}$
Probabilistic k-Means Macqueen (1967) Theorem 9	Shared cluster likelihood by cluster $\sum_{c=1}^m \frac{p(f_\theta(x_i) \text{ and } f_\theta(x_j) \text{ are in cluster } c)}{\mathbb{E}[\text{size of cluster } c]}$	Gaussians on Datapoints, x_i $\frac{\exp(-\ x_i - x_j\ ^2/2\sigma_i^2)}{\sum_{k \neq i} \exp(-\ x_i - x_k\ ^2/2\sigma_i^2)}$
Normalized Cuts Shi & Malik (2000) Theorem 11	Degree-weighted shared cluster likelihood by cluster $\sum_{c=1}^m \frac{p(f_\theta(x_i) \text{ and } f_\theta(x_j) \text{ are in cluster } c) \cdot d_j}{\mathbb{E}[\text{degree of members of cluster } c]}$	Gaussians on edge weights $\frac{\exp(w_{ij}/d_j)}{\sum_k \exp(w_{ik}/d_k)}$
Spectral Clustering Ng et al. (2001) Theorem 5	Shared cluster likelihood by cluster $\sum_{c=1}^m \frac{p(f_\theta(x_i) \text{ and } f_\theta(x_j) \text{ are in cluster } c)}{\mathbb{E}[\text{size of cluster } c]}$	Gaussians on Spectral Embeddings, x_i $\frac{\exp(-\ x_i - x_j\ ^2/2\sigma_i^2)}{\sum_{k \neq i} \exp(-\ x_i - x_k\ ^2/2\sigma_i^2)}$
Mutual Info. Clust. Adaloglou et al. (2023) Theorem 10	Uniform over nearest neighbors $\frac{1}{k} \mathbb{1}[j \text{ is a k-nearest neighbor of } i]$	Shared cluster likelihood by cluster $\sum_{c=1}^m \frac{p(f_\phi(x_i) \text{ and } f_\phi(x_j) \text{ are in cluster } c)}{\mathbb{E}[\text{size of cluster } c]}$
CMC & CLIP Tian et al. (2020) Theorem 6	Uniform over positive pairs from different modalities V $\frac{1}{Z} \mathbb{1}[i \text{ and } j \text{ are positive pairs and } V_i \neq V_j]$	Gaussian based on deep features, $f_\phi(x_i)$ $\frac{\exp(-\ f_\phi(x_i) - f_\phi(x_j)\ ^2)}{\sum_{k \in V_j} \exp(-\ f_\phi(x_i) - f_\phi(x_k)\ ^2)}$
Cross Entropy Good (1963) Corollary 3	Indicator function over Labels $\frac{1}{ C } \mathbb{1}[i \in D \text{ is a data point in a class } j \in C]$	Gaussian based on deep features $\frac{\exp(f_\phi(x_i) \cdot \phi_j)}{\sum_{k \in C} \exp(f_\phi(x_i) \cdot \phi_k)}$
Masked Lang. Modeling Devlin et al. (2019) Corollary 7	Empirical dist. over contexts, i , and tokens, j $\frac{1}{Z} \#[\text{Context } i \text{ precedes token } j]$	Gaussian based on deep features $f_\phi(x_i)$, and token embeddings, ϕ_j $\frac{\exp(f_\phi(x_i) \cdot \phi_j)}{\sum_{k \in C} \exp(f_\phi(x_i) \cdot \phi_k)}$

Table 1: **I-Con unifies representation learners** under different choices of $p_\theta(j|i)$ and $q_\phi(j|i)$.
Proofs of the propositions in this table can be found in the supplement.

216
217

3.1 INFORMATION CONTRASTIVE LEARNING

We begin by defining the mathematical objects of interest. Let $i, j \in \mathcal{X}$ represent two abstract points of a broader set \mathcal{X} . We can then form a probabilistic “neighborhood” around a point j using a function $p(j|i)$. Intuitively, this function measures the probability to “transition” from a point i to another point $j \in \mathcal{X}$. To ensure this function is a proper probability density over \mathcal{X} it should be non-negative: $p(j|i) \geq 0$, and sum to unity: $\int_{j \in \mathcal{X}} p(j|i) = 1$. Here we use the measure-theoretic integral, which includes both the continuous integral and discrete summation depending on the choice of the space \mathcal{X} . Next, we parameterize this neighborhood distribution by abstract parameters, $\theta \in \Theta$. Note that $p_\theta(j|i)$ should be a distribution for all $\theta \in \Theta$. This parameterization transforms p into a *learnable* distribution that can adapt the neighborhoods around each point. Next, let $q_\phi(j|i)$ be a similarly defined family of distributions parameterized by an abstract parameter space $\phi \in \Phi$. With these two families of neighborhood distributions defined we can write the main loss function of I-Con:

230
231
232
233

$$\mathcal{L}(\theta, \phi) = \int_{i \in \mathcal{X}} D_{\text{KL}}(p_\theta(\cdot|i) || q_\phi(\cdot|i)) = \int_{i \in \mathcal{X}} \int_{j \in \mathcal{X}} p_\theta(j|i) \log \frac{p_\theta(j|i)}{q_\phi(j|i)} \quad (1)$$

234
235
236
237
238
239
240
241
242
243
244
245
246
247
248

Where for clarity, D_{KL} , represents the Kullback-Leibler divergence Kullback & Leibler (1951). Intuitively this loss function measures the average similarity between the two parameterized neighborhood distributions and is minimized when $p_\theta(j|i) = q_\phi(j|i)$. In practice, one of the distributions usually p , is set to a fixed “supervisory” distribution with no optimizable parameters θ . We will sometimes omit the parameterization in this case refer to it as $p(j|i)$. In these scenarios the remaining distribution, q_ϕ , is parameterized by a comparison of deep network representations or a comparison of prototypes, clusters, or per-point representations. We illustrate this architecture in Figure 2. Minimizing equation 1 aligns this “learned” distribution q_ϕ to the “supervisory” distribution p by minimizing the average KL divergence between p and q . In the next section, we will show that by selecting different types of parameterized neighborhood distributions p and q , several common methods in the literature emerge as special cases. Interestingly, we note that it is possible to optimize both p_θ and q_ϕ even though no existing methods use this generality. This is an interesting avenue for future study, though we caution that if a uniform distribution is possible in both families of distributions, the optimization will find a trivial solution. Nevertheless, it could be possible to choose the families of distributions p_θ and q_ϕ carefully so that useful behavior emerges.

249
250

3.2 UNIFYING REPRESENTATION LEARNING ALGORITHMS WITH I-CON

251
252
253
254
255
256
257
258
259

Despite the incredible simplicity of Equation 1, this equation is rich enough to generalize several existing methods in the literature simply through the choice of parameterized neighborhood distributions p_θ and q_ϕ . Table 1 summarizes some key choices which recreate popular methods from contrastive learning (SimCLI, MOCOV3, SupCon, CMC, CLIP), dimensionality reduction (SNE, t-SNE), clustering (K-Means, Spectral, TEMI), and supervised learning (Cross-Entropy and Mean Squared Error). Due to limited space, we defer proofs of each of these theorems to the supplemental material. We also note that Table 1 is most certainly not exhaustive, and encourage the community to explore whether other unsupervised learning frameworks implicitly minimize Equation 1 for some choice of p and q .

260
261
262
263
264
265
266
267
268
269

Though there are too many methods unified by I-Con to explain each in detail here, we give an intuitive explanation of how the various choices of p and q generalize SNE and InfoNCE to help the reader gain intuition. The simplest and most direct method to generalize with the I-Con loss is SNE, which was originally phrased as a KL divergence minimization problem. Given a n -dimensional dataset of d vectors, $x \in \mathbb{R}^{d \times n}$, SNE aims to learn a m -dimensional vector representation, $\phi \in \mathbb{R}^{d \times m}$, such that local relationships between high dimensional datapoints are approximately preserved in the low-dimensional representation. The challenge is that the representation dimension, m , is usually much smaller than the data dimensionality n , so the learned representation is significantly constrained. More formally, SNE constructs a probabilistic neighborhood function, $p(j|i)$, around a point x_i , by placing a symmetric Gaussian at x_i and evaluating this distribution at candidate neighbors x_j . It does the same in the low dimensional space to create $q_\phi(j|i)$ by placing a Gaussian at the learned representation vector ϕ_i and comparing to ϕ_j . Finally, SNE learns the

270 representation parameters ϕ to minimize the average KL Divergence, which is exactly the I-Con
 271 loss function.

272 We only need to slightly modify SNE to derive the InfoNCE loss used in contrastive learning ap-
 273 proaches like SimCLR and MocoV3. The first difference is that contrastive learners don't typically
 274 learn a separate representation ϕ_i for every datapoint x_i , but instead learn a parameterized repre-
 275 sentation function $f_\phi(x_i)$ to create representations for data. Secondly, these methods don't rely
 276 on Gaussian neighborhoods in the original data space, instead they use a discrete neighborhood
 277 of known positive pairs for each point x_i . In practice these positive pairs are usually formed by
 278 augmenting or transforming data, such as horizontally flipping or blurring images. When the KL
 279 divergence is taken between this discrete neighborhood and the Gaussian neighborhoods in deep
 280 feature space, we precisely re-derive the InfoNCE loss function. To create MocoV3, we use a stu-
 281 dent model $f_\phi(x_i)$ to featurize a point and an exponential moving averaged teacher model $g(x_j)$ to
 282 represent the neighboring point.

283

284 3.3 CREATING NEW REPRESENTATION LEARNERS WITH I-CON 285

286 I-Con not only allows one to generalize many methods with a single equation but allows one to trans-
 287 fer insights across different domains of representation learning. This allows techniques from one
 288 area, like contrastive learning, to improve methods in another area like clustering. In this work we
 289 show that by surveying modern dimensionality and representation learners we can create new clus-
 290 tering and unsupervised classification methods that perform much better than the prior art. In par-
 291 ticular, we transfer intuitions from spectral clustering, t-SNE, debiased contrastive learning Chuang
 292 et al. (2020) and SCAN to create a state-of-the-art unsupervised image classification system.

293

294 **Adaptive neighborhoods** One key way that t-SNE improves over SNE is to use adaptively sized
 295 neighborhoods around high dimensional points. This allows t-SNE to flexibly adapt its analysis
 296 depending on how densely points are clustered in high dimensional space, effectively eliminating
 297 a key source of hyperparameter tuning in SNE. One way that implementations of t-SNE do this is
 298 by replacing Gaussian neighborhoods with neighborhood distributions based on k-nearest neighbor-
 299 hoods. Similarly, we show in Table 1 shows that by swapping k-Means' Gaussian neighborhoods
 300 to (degree-weighted) KNN neighborhoods we re-derive Spectral clustering, which is well known
 301 for its flexibility and quality. We leverage this insight, and Tables 3 and 4 shows that training a
 302 contrastive learner with KNN-based neighborhood distributions yields a significant improvement on
 303 unsupervised image classification.

304

305 **Debiased Contrastive Learning** addresses the issue that contrastive learning often uses random
 306 points as negative samples, which can overestimate negative terms when the dataset has few un-
 307 derlying classes. Chuang et al. (2020) demonstrate that correcting this bias improves contrastive
 308 representation learning across various backbones and datasets. However, their approach involves
 309 estimating and subtracting false repulsion forces from the loss, increasing attraction forces to create
 310 better feature clusters. This modification results in $q_{j|i}$ no longer being a valid probability distribu-
 311 tion (probabilities do not sum to one) and is difficult to generalize to other domains like clustering
 312 or metric distances.

313

This motivates an alternative debiasing approach inspired by our framework. We aim for: (1) $q_{j|i}$ to
 remain a valid, interpretable conditional distribution representing neighborhoods; (2) adaptability to
 other loss domains like clustering and supervised learning. To achieve this, we introduce uncertainty
 into the supervisory distribution rather than modifying the learned one. For example, in a supervised
 learning setup with cross-entropy loss, this would be equivalent to using soft labels instead of assign-
 ing a probability of 1 to the correct class and 0 to others. The softmax function remains unchanged,
 whereas the method in Chuang et al. (2020) modifies the softmax while keeping hard labels.

319

Therefore, we define a debiased neighborhood added to the original contrastive training neighbor-
 hood $p(j|i)$:

322

323

$$\tilde{p}(j|i) = (1 - \alpha)p(j|i) + \frac{\alpha}{N} \quad (2)$$

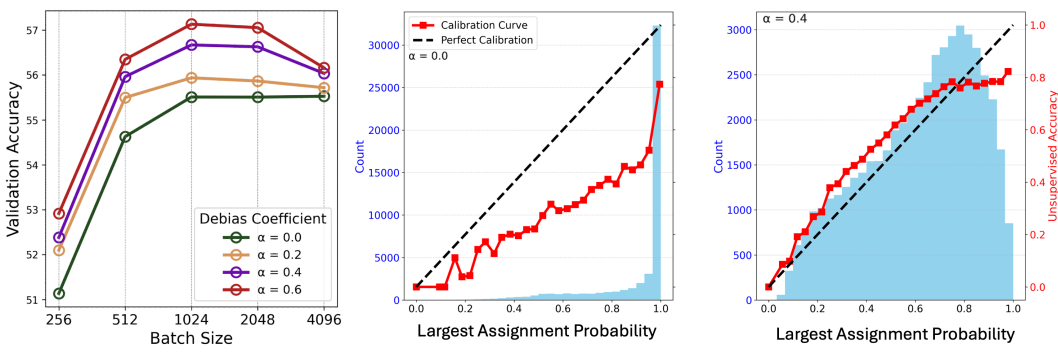


Figure 3: Left: Debiased cluster learning improves performance on ImageNet-1K across batch sizes. Center: Distribution of maximum predicted probabilities for the biased model ($\alpha = 0$) showing poor calibration, with overconfident predictions. Right: Distribution of maximum predicted probabilities for the debiased model ($\alpha = 0.4$), demonstrating improved probability calibration. Debiased training alleviates optimization stiffness by reducing the prevalence of saturated logits, mitigating vanishing gradient issues, and fostering more robust and well-calibrated learning dynamics.

Here, α controls the debiasing amount, and N is the number of points in point i 's neighborhood, ensuring $\tilde{p}(j|i)$ stays normalized. This modification adds $\frac{\alpha}{N}$ probability to each negative pair, counteracting bias effects.

Tables 3 and Figures 4 and 3 show a net positive effect across all experiments and batch sizes. It also relaxes stiff clustering optimization, similar to how label smoothing Szegedy et al. (2016) improves model distillation and generalization. We also explore debiasing both the learned and supervisory distributions, yielding performance improvements. This parallels t-SNE's use of long-tailed Cauchy distributions in learned neighborhoods, aiding optimization to find local minima and avoid saturated solutions with vanishing gradients, as evidenced quantitatively and qualitatively in Figure 3.

Neighbor Propagation as Kernel Smoothing in I-Con Another widespread technique in dimensionality reduction, clustering, and contrastive learning is the use of nearest neighbors in deep feature space to form positive pairs. Within the I-Con framework, this can be seen as an additional form of kernel smoothing. For example, in contrastive learning, the target probabilities can be smoothed by not only considering augmentations but also nearest neighbors in deep feature space. We can also form walks on the nearest neighbor graph similar to the successful Word-Graph2Vec algorithm Li et al. (2023). We refer to this as *neighbor propagation*, and note that it significantly improves performance.

The conditional distribution matrix P , which defines the probability of selecting x_j as a neighbor of x_i (i.e., $P_{ij} = p(x_j|x_i)$), can be interpreted as an adjacency matrix for the training data. A neighbor propagation smoothing of this target distribution is established by considering the number of walks of length at most k between points x_i and x_j :

$$\tilde{P} \propto P + P^2 + \dots + P^k$$

Further smoothing can be applied by transforming the probabilities into a uniform distribution over neighbors reachable within k steps, leading to the following transformation:

$$\tilde{P}_U \propto I[P + P^2 + \dots + P^k > 0]$$

This type of smoothing, based on propagation through nearest neighbors and walk-based approaches, effectively broadens the neighborhood structure considered during learning, allowing the model to capture richer relationships within the data.

4 EXPERIMENTS

The primary objective of this work is to demonstrate that the I-Con framework offers testable hypotheses and practical insights into self-supervised and unsupervised learning. Rather than aiming

only for state-of-the-art performance, our goal is to show how I-Con can enhance existing unsupervised learning methods by leveraging a unified information-theoretic approach. Through this framework, we also highlight the potential for cross-pollination between techniques in varied machine learning domains, such as clustering, contrastive learning, and dimensionality reduction. This transfer of techniques, enabled by I-Con, can significantly improve existing methodologies and open new avenues for exploration.

We focus our experiments on clustering because it is relatively understudied compared to contrastive learning and there are a variety of techniques that can now be adapted to this task. By connecting established methods such as k-Means, SimCLR, and t-SNE within the I-Con framework, we uncover a wide range of possibilities for improving clustering methods. We validate these theoretical insights experimentally, demonstrating the practical impact of I-Con.

We evaluate the I-Con framework using the ImageNet-1K dataset Deng et al. (2009), which consists of 1,000 classes and over one million high-resolution images. This dataset is considered one of the most challenging benchmarks for unsupervised image classification due to its scale and complexity. To ensure fair comparison with prior work, we strictly adhere to the experimental protocol introduced by Adaloglou et al. (2023). The primary metric for evaluating clustering performance is Hungarian Accuracy, which measures the quality of cluster assignments by finding the optimal alignment between predicted clusters and ground truth labels via the Hungarian algorithm Ji et al. (2019). This approach provides a robust measure of clustering performance in an unsupervised context, where direct label supervision is absent during training.

For feature extraction, we utilize the DiNO pre-trained Vision Transformer (ViT) models in three variants: ViT-S/14, ViT-B/14, and ViT-L/14 Caron et al. (2021). These models are chosen to ensure comparability with previous work and to explore how the I-Con framework performs across varying model capacities. The experimental setup, including training protocols, optimization strategies, and data augmentation, mirrors those used in TEMI to ensure consistency in methodology.

The training process involved optimizing a linear classifier on top of the features extracted by the DiNO models. Each model was trained for 30 epochs, using ADAM Kingma & Ba (2017) with batch size of 4096 and an initial learning rate of 1e-3. The learning rate was decayed by a factor of 0.5 every 10 epochs to allow for stable convergence. Notably, no additional normalization was applied to the feature vectors. During training, we applied a variety of data augmentation techniques, including random re-scaling, cropping, color jittering, and Gaussian blurring, to create robust feature representations. Furthermore, to enhance the clustering performance, we pre-computed global nearest neighbors for each image in the dataset using cosine similarity. This allowed us to sample two augmentations and two nearest neighbors for each image in every training batch, thus incorporating both local and global information into the learned representations. We refer to our approach we derived in Table 2 as I-Con. In particular we use a supervisory neighborhood comprised of augmentations, KNNs ($k = 3$), and KNN walks of length 1. We use the “shared cluster likelihood by cluster” neighbourhood from k-Means (See table 1 for Equation) as our learned neighborhood function to drive cluster learning.

4.1 BASELINES

We compare our method against several state-of-the-art clustering methods, including TEMI, SCAN, IIC, and Contrastive Clustering. These methods rely on augmentations and learned representations but often require additional regularization terms or loss adjustments, such as controlling cluster size or reducing the weight of affinity losses. In contrast, our I-Con-based loss function is self-balancing and does not require such manual tuning, making it a cleaner, more theoretically grounded approach. This allows us to achieve higher accuracy and more stable convergence across three different sized backbones.

4.2 RESULTS

Table 2 shows the Hungarian accuracy of I-Con across different DiNO variants (ViT-S/14, ViT-B/14, ViT-L/14) and compares it with several state-of-the-art clustering methods. The I-Con framework consistently outperforms the other state-of-the-art methods across all model sizes. Specifically, for the DiNO ViT-B/14 and ViT-L/14 models, I-Con achieves significant performance gains of +4.5%

Method	DiNO ViT-S/14	DiNO ViT-B/14	DiNO ViT-L/14
k-Means	51.84	52.26	53.36
Contrastive Clustering	47.35	55.64	59.84
SCAN	49.20	55.60	60.15
TEMI	56.84	58.62	—
InfoNCE Clustering (Ours)	57.8 ± 0.26	64.75 ± 0.18	67.52 ± 0.28

Table 2: Comparison of methods on ImageNet-1K clustering with respect to Hungarian Accuracy. I-Con significantly outperforms the prior state-of-the-art TEMI. Note that TEMI does not report results for ViT-L.

Method	DiNO ViT-S/14	DiNO ViT-B/14	DiNO ViT-L/14
Baseline	55.51	63.03	65.70
+ Debiasing	57.27 ± 0.07	63.72 ± 0.09	66.87 ± 0.07
+ KNN Propagation	58.45 ± 0.23	64.87 ± 0.19	67.25 ± 0.21
+ EMA	57.8 ± 0.26	64.75 ± 0.18	67.52 ± 0.28

Table 3: Ablation study of new techniques discovered through the I-Con framework. We compare ImageNet-1K clustering accuracy across different sized backbones.

Method	DiNO ViT-S/14	DiNO ViT-B/14	DiNO ViT-L/14
Baseline	55.51	63.03	65.72
+ KNNs	56.43	64.26	65.70
+ 1-walks on KNN	58.09	64.29	65.97
+ 2-walks on KNN	57.84	64.27	67.26
+ 3-walks on KNN	57.82	64.15	67.02

Table 4: Ablation Study on Neighbor Propagation. Adding both KNNs and walks of length 1 or 2 on the KNN graph achieves the best performance.

and +7.8% in Hungarian accuracy compared to TEMI, the prior state-of-the-art ImageNet clusterer. The improvements in performance can be attributed to two main factors:

Self-Balancing Loss: Unlike TEMI or SCAN, which require hand-tuned regularizations (e.g., balancing cluster sizes or managing the weight of affinity losses), I-Con’s loss function automatically balances these factors without additional regularization hyper-parameter tuning as we are using the exact same clustering kernel used by k-Means. This theoretical underpinning leads to more robust and accurate clusters.

Cross-Domain Insights: I-Con leverages insights from contrastive learning to refine clustering by looking at pairs of images based on their embeddings, treating augmentations and neighbors similarly. This approach, originally successful in contrastive learning, translates well into clustering and leads to improved performance in high-dimensional, noisy image data.

4.3 ABLATIONS

We conduct several ablation studies to experimentally justify the architectural improvements that emerged from analyzing contrastive clustering through the I-Con framework. These ablations focus on two key areas: the effect of incorporating debiasing into the target and embedding spaces and the impact of neighbor propagation strategies which are both kernel smoothing methods.

We perform experiments with different levels of debiasing in the target distribution, denoted by the parameter α , and test configurations where debiasing is applied on either the target side, both sides (target and learned representations), or none. As seen in Figure 4, adding debiasing improves performance, with the optimal value typically around $\alpha = 0.6$ to $\alpha = 0.8$, particularly when applied to both sides of the learning process. This method is similar to how debiasing work in contrastive

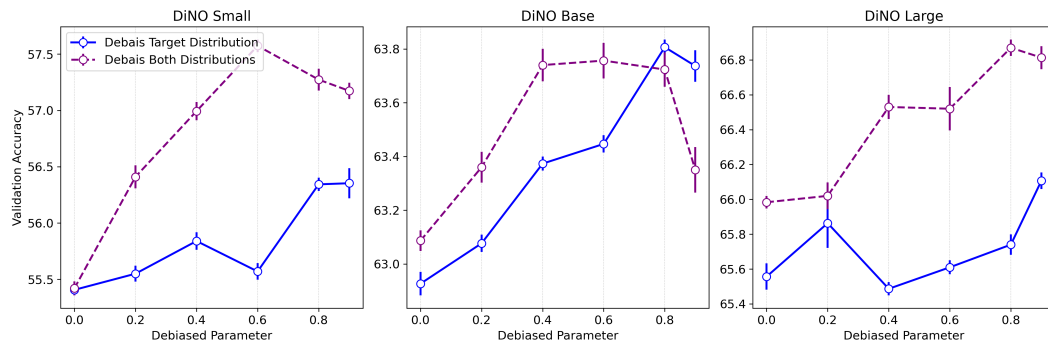


Figure 4: Effects of increasing the debias weight α on the supervisory neighborhood (blue line) and both the learned and supervisory neighborhood (red line). Adding some amount of debiasing helps in all cases, with a double debiasing yielding the largest improvements.

learning by assuming that each negative sample has a non-zero probability (α/N) of being incorrect. Figure 3 shows how changing the value of α improves performance across different batch sizes.

In a second set of experiments, shown in Table 4, we examine the impact of neighbor propagation strategies. We evaluate clustering performance when local and global neighbors are included in the contrastive loss computation. Neighbor propagation, especially at small scales ($s = 1$ and $s = 2$), significantly boosts performance across all model sizes, showing the importance of capturing local structure in the embedding space. Larger neighbor propagation values (e.g., $s = 3$) offer diminishing returns, suggesting that over-propagating neighbors may dilute the information from the nearest, most relevant points. Note that only DiNO-L/14 showed preference for large step size, and this is likely due to its higher k-nearest neighbor ability, so the augmented links are correct.

Our ablation studies highlight that small adjustments in the debiasing parameter and neighbor propagation can lead to notable improvements that achieve a state-of-the-art result with a simple loss function. Additionally, sensitivity to α and propagation size varies across models, with larger models generally benefiting more from increased propagation but requiring fine-tuning of α for optimal performance. We recommend using $\alpha \approx 0.6$ to $\alpha \approx 0.8$ and limiting neighbor propagation to small values for a balance between performance and computational efficiency.

5 CONCLUSION

In summary, we have developed I-Con: a single information theoretic equation that unifies a broad class of machine learning methods. We provided over 9 theorems that prove this assertion for many of the most popular loss functions used in clustering, spectral graph theory, supervised and unsupervised contrastive learning, dimensionality reduction, and supervised classification and regression. We not only theoretically unify these algorithms but show that our connections can help us discover new state-of-the-art methods, and apply improvements discovered for a particular method to any other method in the class. We illustrate this by creating a new method for unsupervised image classification that achieves a +8% improvement over the prior art. We believe that the results presented in this work represent just a fraction of the methods that are potentially unify-able with I-Con, and we hope the community can use this viewpoint to improve collaboration and analysis across algorithms and machine learning disciplines.

REFERENCES

- Nikolas Adaloglou, Felix Michels, Hamza Kalisch, and Markus Kollmann. Exploring the limits of deep image clustering using pretrained models. *arXiv preprint arXiv:2303.17896*, 2023.
- Philip Bachman, R Devon Hjelm, and William Buchwalter. Learning representations by maximizing mutual information across views. *Advances in neural information processing systems*, 32, 2019.

- 540 Randall Balestrier and Yann LeCun. Contrastive and non-contrastive self-supervised learning re-
 541 cover global and local spectral embedding methods. *Advances in Neural Information Processing*
 542 *Systems*, 35:26671–26685, 2022.
- 543
- 544 Yoshua Bengio, Aaron Courville, and Pascal Vincent. Representation learning: A review and new
 545 perspectives. *IEEE transactions on pattern analysis and machine intelligence*, 35(8):1798–1828,
 546 2013.
- 547 David M Blei, Alp Kucukelbir, and Jon D McAuliffe. Variational inference: A review for statisti-
 548 cians. *Journal of the American statistical Association*, 112(518):859–877, 2017.
- 549
- 550 Jan Niklas Böhm, Philipp Berens, and Dmitry Kobak. Unsupervised visualization of image datasets
 551 using contrastive learning. *arXiv preprint arXiv:2210.09879*, 2022.
- 552
- 553 Mathilde Caron, Hugo Touvron, Ishan Misra, Hervé Jégou, Julien Mairal, Piotr Bojanowski, and
 554 Armand Joulin. Emerging properties in self-supervised vision transformers, 2021. URL <https://arxiv.org/abs/2104.14294>.
- 555
- 556 Ting Chen, Simon Kornblith, Mohammad Norouzi, and Geoffrey Hinton. A simple framework for
 557 contrastive learning of visual representations. In *International conference on machine learning*,
 558 pp. 1597–1607. PMLR, 2020a.
- 559
- 560 Xinlei Chen, Haoqi Fan, Ross Girshick, and Kaiming He. Improved baselines with momentum
 561 contrastive learning. *arXiv preprint arXiv:2003.04297*, 2020b.
- 562
- 563 Xinlei Chen*, Saining Xie*, and Kaiming He. An empirical study of training self-supervised vision
 564 transformers. *arXiv preprint arXiv:2104.02057*, 2021.
- 565
- 566 Ching-Yao Chuang, Joshua Robinson, Lin Yen-Chen, Antonio Torralba, and Stefanie Jegelka. De-
 567 biased contrastive learning, 2020. URL <https://arxiv.org/abs/2007.00224>.
- 568
- 569 Keenan Crane, Clarisse Weischedel, and Max Wardetzky. Geodesics in heat: A new approach to
 570 computing distance based on heat flow. *ACM Transactions on Graphics (TOG)*, 32(5):1–11, 2013.
- 571
- 572 Arthur P Dempster, Nan M Laird, and Donald B Rubin. Maximum likelihood from incomplete data
 573 via the em algorithm. *Journal of the royal statistical society: series B (methodological)*, 39(1):
 574 1–22, 1977.
- 575
- 576 Jia Deng, Wei Dong, Richard Socher, Li-Jia Li, Kai Li, and Li Fei-Fei. Imagenet: A large-scale hi-
 577 erarchical image database. In *2009 IEEE conference on computer vision and pattern recognition*,
 578 pp. 248–255. Ieee, 2009.
- 579
- 580 Jacob Devlin, Ming-Wei Chang, Kenton Lee, and Kristina Toutanova. Bert: Pre-training of deep
 581 bidirectional transformers for language understanding, 2019. URL <https://arxiv.org/abs/1810.04805>.
- 582
- 583 Wouter Van Gansbeke, Simon Vandenhende, Stamatios Georgoulis, Marc Proesmans, and Luc Van
 584 Gool. Scan: Learning to classify images without labels, 2020. URL <https://arxiv.org/abs/2005.12320>.
- 585
- 586 Irving J Good. Maximum entropy for hypothesis formulation, especially for multidimensional con-
 587 tingency tables. *The Annals of Mathematical Statistics*, pp. 911–934, 1963.
- 588
- 589 Roger Grosse, Ruslan R Salakhutdinov, William T Freeman, and Joshua B Tenenbaum. Exploiting
 590 compositionality to explore a large space of model structures. *arXiv preprint arXiv:1210.4856*,
 591 2012.
- 592
- 593 Geoffrey E Hinton and Sam Roweis. Stochastic neighbor embedding. *Advances in neural informa-
 594 tion processing systems*, 15, 2002.
- Tianyang Hu, Zhili Liu, Fengwei Zhou, Wenjia Wang, and Weiran Huang. Your contrastive learning
 is secretly doing stochastic neighbor embedding. *arXiv preprint arXiv:2205.14814*, 2022.

- 594 Xu Ji, Joao F Henriques, and Andrea Vedaldi. Invariant information clustering for unsupervised
 595 image classification and segmentation. In *Proceedings of the IEEE/CVF international conference*
 596 *on computer vision*, pp. 9865–9874, 2019.
- 597
- 598 Prannay Khosla, Piotr Teterwak, Chen Wang, Aaron Sarna, Yonglong Tian, Phillip Isola, Aaron
 599 Maschinot, Ce Liu, and Dilip Krishnan. Supervised contrastive learning. *Advances in neural*
 600 *information processing systems*, 33:18661–18673, 2020.
- 601 Diederik P. Kingma and Jimmy Ba. Adam: A method for stochastic optimization, 2017. URL
 602 <https://arxiv.org/abs/1412.6980>.
- 603
- 604 Alex Krizhevsky, Ilya Sutskever, and Geoffrey E Hinton. Imagenet classification with deep convo-
 605 lutional neural networks. *Communications of the ACM*, 60(6):84–90, 2017.
- 606 Joseph B Kruskal. Multidimensional scaling by optimizing goodness of fit to a nonmetric hypothe-
 607 sis. *Psychometrika*, 29(1):1–27, 1964.
- 608
- 609 Solomon Kullback and Richard A Leibler. On information and sufficiency. *The annals of mathe-
 610 matical statistics*, 22(1):79–86, 1951.
- 611
- 612 Phuc H Le-Khac, Graham Healy, and Alan F Smeaton. Contrastive representation learning: A
 613 framework and review. *Ieee Access*, 8:193907–193934, 2020.
- 614
- 615 Wenting Li, Jiahong Xue, Xi Zhang, Huacan Chen, Zeyu Chen, Feijuan Huang, and Yuanzhe Cai.
 616 Word-graph2vec: An efficient word embedding approach on word co-occurrence graph using
 617 random walk technique, 2023. URL <https://arxiv.org/abs/2301.04312>.
- 618
- 619 Yunfan Li, Peng Hu, Zitao Liu, Dezhong Peng, Joey Tianyi Zhou, and Xi Peng. Contrastive cluster-
 620 ing. In *Proceedings of the AAAI conference on artificial intelligence*, volume 35, pp. 8547–8555,
 621 2021.
- 622
- 623 J Macqueen. Some methods for classification and analysis of multivariate observations. In *Pro-
 624 ceedings of 5-th Berkeley Symposium on Mathematical Statistics and Probability/University of
 California Press*, 1967.
- 625
- 626 Leland McInnes, John Healy, and James Melville. Umap: Uniform manifold approximation and
 627 projection for dimension reduction. *arXiv preprint arXiv:1802.03426*, 2018.
- 628
- 629 Andrew Ng, Michael Jordan, and Yair Weiss. On spectral clustering: Analysis and an algorithm.
Advances in neural information processing systems, 14, 2001.
- 630
- 631 Aaron van den Oord, Yazhe Li, and Oriol Vinyals. Representation learning with contrastive predic-
 632 tive coding. *arXiv preprint arXiv:1807.03748*, 2018.
- 633
- 634 Karl Pearson. Liii. on lines and planes of closest fit to systems of points in space. *The London,
 Edinburgh, and Dublin philosophical magazine and journal of science*, 2(11):559–572, 1901.
- 635
- 636 Ben Poole, Sherjil Ozair, Aaron Van Den Oord, Alex Alemi, and George Tucker. On variational
 637 bounds of mutual information. In *International Conference on Machine Learning*, pp. 5171–
 638 5180. PMLR, 2019.
- 639
- 640 Alec Radford, Jong Wook Kim, Chris Hallacy, Aditya Ramesh, Gabriel Goh, Sandhini Agar-
 641 wal, Girish Sastry, Amanda Askell, Pamela Mishkin, Jack Clark, Gretchen Krueger, and Ilya
 642 Sutskever. Learning transferable visual models from natural language supervision, 2021. URL
<https://arxiv.org/abs/2103.00020>.
- 643
- 644 Florian Schroff, Dmitry Kalenichenko, and James Philbin. Facenet: A unified embedding for face
 645 recognition and clustering. In *Proceedings of the IEEE conference on computer vision and pattern
 646 recognition*, pp. 815–823, 2015.
- 647
- Jianbo Shi and Jitendra Malik. Normalized cuts and image segmentation. *IEEE Transactions on
 pattern analysis and machine intelligence*, 22(8):888–905, 2000.

- 648 Christian Szegedy, Vincent Vanhoucke, Sergey Ioffe, Jon Shlens, and Zbigniew Wojna. Rethink-
649 ing the inception architecture for computer vision. In *Proceedings of the IEEE conference on*
650 *computer vision and pattern recognition*, pp. 2818–2826, 2016.
- 651
- 652 Yonglong Tian, Dilip Krishnan, and Phillip Isola. Contrastive multiview coding. In *Computer*
653 *Vision–ECCV 2020: 16th European Conference, Glasgow, UK, August 23–28, 2020, Proceedings,*
654 *Part XI 16*, pp. 776–794. Springer, 2020.
- 655 Michael Tschannen, Josip Djolonga, Paul K Rubenstein, Sylvain Gelly, and Mario Lucic. On mutual
656 information maximization for representation learning. *arXiv preprint arXiv:1907.13625*, 2019.
- 657
- 658 Laurens Van der Maaten and Geoffrey Hinton. Visualizing data using t-sne. *Journal of machine*
659 *learning research*, 9(11), 2008.
- 660
- 661 Lilian Weng. Contrastive representation learning. *lilianweng.github.io*, May 2021. URL <https://lilianweng.github.io/posts/2021-05-31-contrastive/>.
- 662
- 663 Jianwei Yang, Chunyuan Li, Pengchuan Zhang, Bin Xiao, Ce Liu, Lu Yuan, and Jianfeng Gao. Uni-
664 fied contrastive learning in image-text-label space. In *Proceedings of the IEEE/CVF Conference*
665 *on Computer Vision and Pattern Recognition*, pp. 19163–19173, 2022.
- 666
- 667
- 668
- 669
- 670
- 671
- 672
- 673
- 674
- 675
- 676
- 677
- 678
- 679
- 680
- 681
- 682
- 683
- 684
- 685
- 686
- 687
- 688
- 689
- 690
- 691
- 692
- 693
- 694
- 695
- 696
- 697
- 698
- 699
- 700
- 701

702 A ADDITIONAL EXPERIMENTS 703

704 The following experiments aim to test the effect of our debiasing approach in feature learning. We
705 followed the experimental setup introduced by Hu et al. Hu et al. (2022). The architecture consisted
706 of a ResNet-34 backbone paired with a two-layer multilayer perceptron (MLP) feature extractor.
707 The MLP included a hidden layer with 512 units and an output layer with 64 units, without batch
708 normalization.

709 **CIFAR-10 & CIFAR-100.** The models were trained on the CIFAR-10 dataset for 1000 epochs
710 using the AdamW optimizer with the following hyperparameters: $\beta_1 = 0.9$, $\beta_2 = 0.999$, a learning
711 rate of 1×10^{-3} , a batch size of 1024, and a weight decay of 1×10^{-5} . The learned kernel was
712 either Gaussian or Student’s t-distribution with degrees of freedom $d_f = 2$.

713 For evaluation, we used two methods: (1) linear probing on the 512-dimensional embeddings from
714 the MLP’s hidden layer, and (2) k -nearest neighbors ($k = 3$) classification based on the same
715 embeddings for CIFAR-10 (in-distribution) and CIFAR-100 (out-of-distribution).

716 **STL-10 & Oxford-IIIT Pet.** With a similar setup, the models were trained contrastively on STL-10
717 (in distribution) without labels using the same hyperparameters as in the CIFAR experiments. For
718 evaluation, we performed (1) linear probing for the STL-10 classification task and Oxford-IIIT Pet
719 binary classification, and (2) k -nearest neighbors classification based on the same embeddings for
720 STL-10 and Oxford-IIIT Pet with $k = 10$.

722 Method	723 CIFAR10 (in distribution)		724 CIFAR100 (out of distribution)	
	725 Linear Probing	KNN	Linear Probing	KNN
q_ϕ is a Gaussian Distribution				
726 SimCLR Chen et al. (2020a)	77.79	80.02	31.82	40.27
727 DCL Chuang et al. (2020)	78.32	83.11	32.44	42.10
Our Debiasing $\alpha = 0.2$	79.50	84.07	32.53	43.19
Our Debiasing $\alpha = 0.4$	79.07	85.06	32.53	43.29
Our Debiasing $\alpha = 0.6$	79.32	85.90	30.67	29.79
q_ϕ is a Student’s t-distribution				
732 t-SimCLRHu et al. (2022)	90.97	88.14	38.96	30.75
733 DCL Chuang et al. (2020)	Diverges	Diverges	Diverges	Diverges
Our Debiasing $\alpha = 0.2$	91.31	88.34	41.62	32.88
Our Debiasing $\alpha = 0.4$	92.70	88.50	41.98	34.26
Our Debiasing $\alpha = 0.6$	92.86	88.92	38.92	32.51

731 Table 5: Contrastive feature learning evaluation results for CIFAR10 and CIFAR100 datasets with
732 various debasing α factors. Adding some amount of debasing helps raising accuracy in both linear
733 probing and KNN classification.

742 Method	743 STL-10 (in distribution)		744 Oxford-IIIT Pet (out of distribution)	
	745 Linear Probing	KNN	746 Logistic Regression	KNN
747 SimCLR Chen et al. (2020a)	77.71	74.92	74.80	71.48
DCL Chuang et al. (2020)	78.32	75.03	74.41	70.22
q_ϕ is a Student’s t-distribution				
748 t-SimCLRHu et al. (2022)	85.11	83.05	83.40	81.41
Our Debiasing $\alpha = 0.2$	85.94	83.15	84.11	81.15
Our Debiasing $\alpha = 0.4$	86.13	84.14	84.07	84.13
Our Debiasing $\alpha = 0.6$	87.18	83.58	84.51	83.04

753 Table 6: Contrastive feature learning evaluation results for STL10 (in distribution) and Oxford-
754 IIIT Pet (out of distribution) with various debasing α factors. Similar to the other experiments, our
755 debasing helps raising accuracy in both linear probing and KNN classification.

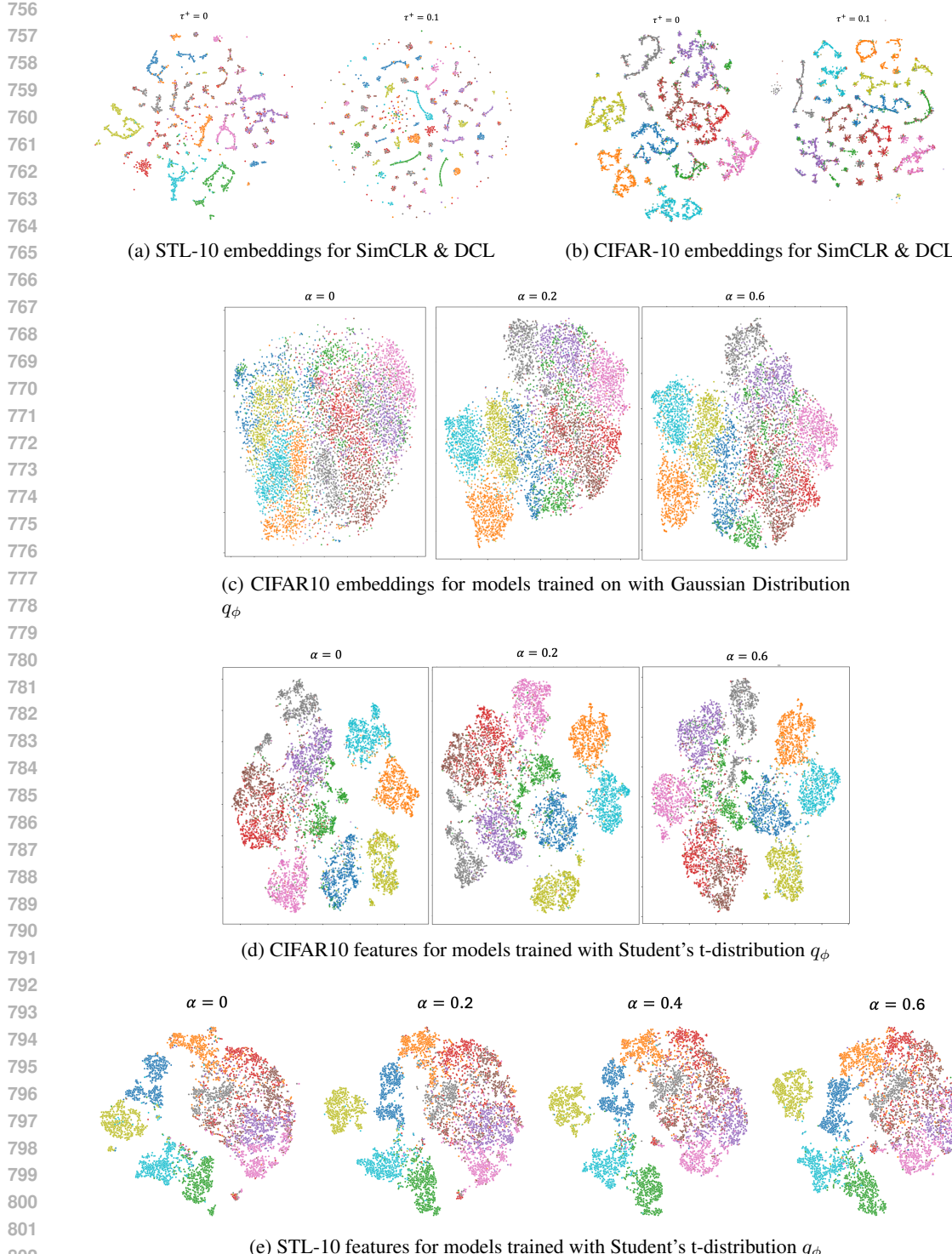


Figure 5: t-SNE visualizations of learned embeddings on CIFAR10 and STL10 datasets. (a) and (b) display embeddings from the DCL Chuang et al. (2020) method before and after applying debiasing, showing a tendency to heavily cluster data points, which may hinder out-of-distribution generalization Hu et al. (2022). (c) and (d) show embeddings with Student’s t-distribution, where the debiasing factor α enhances clustering and separation, resulting in improved data representation.

810 B UNIFYING DIMENSIONALITY REDUCTION METHODS 811

812 We begin by defining the setup for dimensionality reduction methods in the context of I-Con. Let
813 $x_i \in \mathbb{R}^d$ represent high-dimensional data points, and $\phi_i \in \mathbb{R}^m$ represent their corresponding low-
814 dimensional embeddings, where $m \ll d$. The goal of dimensionality reduction methods, such as
815 Stochastic Neighbor Embedding (SNE) and t-Distributed Stochastic Neighbor Embedding (t-SNE),
816 is to learn these embeddings such that neighborhood structures in the high-dimensional space are
817 preserved in the low-dimensional space. In this context, the low-dimensional embeddings ϕ_i can
818 be interpreted as the outputs of a mapping function $f_\theta(x_i)$, where f_θ is essentially an embedding
819 matrix or look-up table. The I-Con framework is well-suited to express this relationship through a
820 KL divergence loss between two neighborhood distributions: one in the high-dimensional space and
821 one in the low-dimensional space.

822 **Theorem 1.** *Stochastic Neighbor Embedding (SNE) Hinton & Roweis (2002) is an instance of the
823 I-Con framework.*

824 *Proof.* This is one of the most straightforward proofs in this paper, essentially based on the definition
825 of SNE. The target distribution (supervised part), described by the neighborhood distribution in the
826 high-dimensional space, is given by:

$$827 p_\theta(j|i) = \frac{\exp(-\|x_i - x_j\|^2/2\sigma_i^2)}{\sum_{k \neq i} \exp(-\|x_i - x_k\|^2/2\sigma_i^2)},$$

830 while the learned low-dimensional neighborhood distribution is:

$$831 q_\phi(j|i) = \frac{\exp(-\|\phi_i - \phi_j\|^2)}{\sum_{k \neq i} \exp(-\|\phi_i - \phi_k\|^2)}.$$

834 The objective is to minimize the KL divergence between these distributions:

$$835 \mathcal{L} = \sum_i D_{\text{KL}}(p_\theta(\cdot|i) \| q_\phi(\cdot|i)) = \sum_i \sum_j p_\theta(j|i) \log \frac{p_\theta(j|i)}{q_\phi(j|i)}.$$

838 The embeddings θ_i are learned implicitly by minimizing \mathcal{L} . The mapper is an embedding matrix,
839 as SNE is a non-parametric optimization. Therefore, SNE is a special case of the I-Con framework,
840 where $p_\theta(j|i)$ and $q_\phi(j|i)$ represent the neighborhood probabilities in the high- and low-dimensional
841 spaces, respectively. \square

843 **Theorem 2** (t-SNE Van der Maaten & Hinton (2008)). *t-SNE is an instance of the I-Con framework.*

845 *Proof.* The proof is similar to the one for SNE. While the high-dimensional target distribution
846 $p_\theta(j|i)$ remains unchanged, t-SNE modifies the low-dimensional distribution to a Student's t-
847 distribution with one degree of freedom (Cauchy distribution):

$$848 q_\phi(j|i) = \frac{(1 + \|\phi_i - \phi_j\|^2)^{-1}}{\sum_{k \neq i} (1 + \|\phi_i - \phi_k\|^2)^{-1}}.$$

851 The objective remains to minimize the KL divergence. Therefore, t-SNE is an instance of the I-Con
852 framework. \square

853 **Proposition 1.** *Let $X := \{x_i\}_{i=1}^n$, then the following cohesion variance loss*

$$855 \mathcal{L} = \frac{1}{n} \sum_{ij} w_{ij} \|f_\phi(x_i) - f_\phi(x_j)\|^2 - 2\text{Var}(X)$$

857 is an instance of I-Con in the special case $w_{ij} = p(j|i)$ and q_ϕ is Gaussian as with a large width
858 as $\sigma \rightarrow \infty$.

860 *Proof.* By using AM-GM inequality, we have

$$862 \frac{1}{n} \sum_{k=1}^n e^{-z_k} \geq (\prod_{k=1}^n e^{-z_k})^{\frac{1}{n}} \implies \frac{1}{n} \sum_{k=1}^n e^{-z_k} \geq (e^{-\sum_{k=1}^n z_k})^{\frac{1}{n}}$$

864 which implies that
 865

$$866 \quad \log \sum_{k=1}^n e^{-z_k} - \log n \geq \log \left(e^{-\sum_{k=1}^n z_k} \right)^{\frac{1}{n}} \implies \log \sum_{k=1}^n e^{-z_k} \geq -\frac{1}{n} \sum_{k=1}^n z_k + \log(n)$$

869
 870 Alternatively, this can be written as
 871

$$872 \quad -\log \sum_{k=1}^n e^{-z_k} \leq \frac{1}{n} \sum_{k=1}^n z_k - \log(n)$$

875 Now assume that we have a Gaussian Kernel q_ϕ
 876

$$877 \quad q_\phi(j|i) = \frac{\exp(-\|f_\phi(x_i) - f_\phi(x_j)\|^2/\sigma^2)}{\sum_{k \neq i} \exp(-\|f_\phi(x_i) - f_\phi(x_k)\|^2/\sigma^2)},$$

880 Therefore, given the inequality of exp-sum that we showed above, we have
 881

$$882 \quad \log q_\phi(j|i) = -\frac{\|f_\phi(x_i) - f_\phi(x_j)\|^2}{\sigma^2} - \log \sum_{k \neq i} \exp\left(-\frac{\|f_\phi(x_i) - f_\phi(x_k)\|^2}{\sigma^2}\right)$$

$$883 \quad \leq -\frac{1}{\sigma^2} \|f_\phi(x_i) - f_\phi(x_j)\|^2 + \frac{1}{n\sigma^2} \sum_{k \neq i} \|f_\phi(x_i) - f_\phi(x_k)\|^2 - \log(n)$$

$$884 \quad = -\frac{1}{\sigma^2} (-\|f_\phi(x_i) - f_\phi(x_j)\|^2 + \frac{1}{n} \sum_{k \neq i} \|f_\phi(x_i) - f_\phi(x_k)\|^2) - \log(n)$$

890
 891 Therefore, the cross entropy $H(p_\theta, q_\phi)$, is bounded by
 892

$$893 \quad H(p_\theta, q_\phi) = -\frac{1}{n} \sum_i \sum_j p(j|i) \log q_\phi(j|i)$$

$$894 \quad \leq \frac{1}{n} \sum_i \sum_j p(j|i) \left(\frac{1}{\sigma^2} (-\|f_\phi(x_i) - f_\phi(x_j)\|^2 + \frac{1}{n} \sum_{k \neq i} \|f_\phi(x_i) - f_\phi(x_k)\|^2) - \log(n) \right)$$

$$895 \quad = \frac{1}{\sigma^2} \left(\frac{1}{n} \sum_{ij} p(j|i) \|f_\phi(x_i) - f_\phi(x_j)\|^2 - \frac{1}{n^2} \sum_{ijk} p(j|i) \|f_\phi(x_i) - f_\phi(x_k)\|^2 \right) - \log(n)$$

$$896 \quad = \frac{1}{\sigma^2} \left(\frac{1}{n} \sum_{ij} p(j|i) \|f_\phi(x_i) - f_\phi(x_j)\|^2 - 2\text{Var}(X) \right) + \log(n)$$

907
 908 On the other hand, when $z \approx 0$, the L.H.S. can be upper bounded by using second order bound
 909 $e^{-z} \leq 1 - z + z^2/2$, which implies that
 910

$$911 \quad -\log \sum_{k=1}^n e^{-z_k} \geq \log(1 - \frac{1}{n} \sum_{k=1}^n z_k + \frac{1}{n} \sum_{k=1}^n z_k^2) - \log(n)$$

914 Therefore, in the limit $\sigma \rightarrow \infty$, the bounds become tighter and the I-Con loss approaches the
 915 cohesion variance loss. \square
 916

917 **Corollary 1.** Principal Component Analysis (PCA) is an asymptotic instance of the I-Con.

918 *Proof.* There are two ways to prove this result. One is by using Proposition 1. When $p_{j|i} = \mathbf{1}[i = j]$,
 919 we have the following expression for \mathcal{L}

$$\begin{aligned} 921 \quad \mathcal{L} &= \frac{1}{n} \sum_{ij} p_{j|i} \|f_\phi(x_i) + f_\phi(x_j)\|^2 - 2\text{Var}(X) \\ 922 \\ 923 \quad &= \frac{1}{n} \sum_i \|f_\phi(x_i) - f_\phi(x_i)\|^2 - 2\text{Var}(X) \\ 924 \\ 925 \quad &= -2\text{Var}(X) \\ 926 \\ 927 \end{aligned}$$

928 Therefore, minimizing \mathcal{L} is equivalent to maximizing the variance which is the equivalent of the PCA
 929 objective. Intuitively, the KL divergence is asking $-\|f_\phi(x_i) - f_\phi(x_j)\|^2 = 0$ to be the maximum in
 930 comparison to $-\|f_\phi(x_i) - f_\phi(x_j)\|^2$ to match the supervisory indicator function, which implies the
 931 minimization of the sum of $-\|f_\phi(x_i) - f_\phi(x_j)\|^2$, which is maximizing the variance. \square

932 **Theorem 3.** *Multidimensional Scaling (MDS) is an asymptotic instance of the I-Con framework.*

933 *Proof.* MDS aims to find embeddings $f_\phi(x_i)$ that preserve the original pairwise distances $d_{ij} =$
 934 $\|x_i - x_j\|$. The classical MDS objective minimizes:

$$\mathcal{L}_{\text{MDS}} = \sum_{i,j} (\|f_\phi(x_i) - f_\phi(x_j)\|^2 - d_{ij}^2)^2.$$

935 In the I-Con framework, define the target distribution based on the original distances:

$$\begin{aligned} 936 \quad p_\theta(j|i) &= \frac{\exp\left(-\frac{d_{ij}^2}{\sigma^2}\right)}{\sum_k \exp\left(-\frac{d_{ik}^2}{\sigma^2}\right)}. \\ 937 \end{aligned}$$

938 Similarly, the learned distribution is:

$$\begin{aligned} 939 \quad q_\phi(j|i) &= \frac{\exp\left(-\frac{\|f_\phi(x_i) - f_\phi(x_j)\|^2}{\sigma^2}\right)}{\sum_k \exp\left(-\frac{\|f_\phi(x_i) - f_\phi(x_k)\|^2}{\sigma^2}\right)}. \\ 940 \end{aligned}$$

941 For large σ , we approximate:

$$\exp\left(-\frac{z}{\sigma^2}\right) \approx 1 - \frac{z}{\sigma^2}.$$

942 Substituting into $p_\theta(j|i)$ and $q_\phi(j|i)$, the denominators become constants. The I-Con loss simplifies
 943 to:

$$\begin{aligned} 944 \quad \mathcal{L} &= - \sum_{i,j} p_\theta(j|i) \log q_\phi(j|i) \\ 945 \\ 946 \quad &\approx \frac{1}{\sigma^2} \sum_{i,j} p_\theta(j|i) (\|f_\phi(x_i) - f_\phi(x_j)\|^2 - \text{const}). \\ 947 \end{aligned}$$

948 Neglecting constants and considering symmetric $p_\theta(j|i)$, minimizing \mathcal{L} corresponds to minimizing:

$$\sum_{i,j} p_\theta(j|i) \|f_\phi(x_i) - f_\phi(x_j)\|^2.$$

949 Since $p_\theta(j|i)$ reflects the original distances d_{ij} , this objective aligns with preserving the pairwise
 950 distances in the embedding space, as in MDS. Therefore, MDS is an asymptotic instance of the
 951 I-Con framework when σ is large. \square

972 C UNIFYING FEATURE LEARNING METHODS 973

974 We now extend the I-Con framework to feature learning methods commonly used in contrastive
975 learning. Let $x_i \in \mathbb{R}^d$ be the input data points, and $f_\phi(x_i) \in \mathbb{R}^m$ be their learned feature embedding.
976 In contrastive learning, the goal is to learn these embeddings such that similar data points
977 (positive pairs) are close in the embedding space, while dissimilar points (negative pairs) are far
978 apart. This setup can be expressed using a neighborhood distribution in the original space, where
979 "neighbors" are defined not by proximity in Euclidean space, but by predefined relationships such
980 as data augmentations or class membership. The learned embeddings $f_\phi(x_i)$ define a new distribution
981 over neighbors, typically using a Gaussian kernel in the learned feature space. We show that
982 InfoNCE is a natural instance of the I-Con framework, and many other methods, such as SupCon,
983 CMC, and Cross Entropy, follow from this.

984 **Theorem 4** (InfoNCE Bachman et al. (2019)). *InfoNCE is an instance of the I-Con framework.*

985
986 *Proof.* InfoNCE aims to maximize the similarity between positive pairs while minimizing it for
987 negative pairs in the learned feature space. In the I-Con framework, this can be interpreted as
988 minimizing the divergence between two distributions: the neighborhood distribution in the original
989 space and the learned distribution in the embedding space.

990 The neighborhood distribution $p_\theta(j|i)$ is uniform over the positive pairs, defined as:

$$992 p_\theta(j|i) = \begin{cases} \frac{1}{k} & \text{if } x_j \text{ is among the } k \text{ positive views of } x_i, \\ 993 0 & \text{otherwise.} \end{cases}$$

994 where k is the number of positive pairs for x_i .

995 The learned distribution $q_\phi(j|i)$ is based on the similarities between the embeddings $f_\phi(x_i)$ and
996 $f_\phi(x_j)$, constrained to unit norm ($\|f_\phi(x_i)\| = 1$). Using a temperature-scaled Gaussian kernel, this
997 distribution is given by:

$$1000 q_\phi(j|i) = \frac{\exp(f_\phi(x_i) \cdot f_\phi(x_j)/\tau)}{1001 \sum_{k \neq i} \exp(f_\phi(x_i) \cdot f_\phi(x_k)/\tau)},$$

1002 where τ is the temperature parameter controlling the sharpness of the distribution. Since $\|f_\phi(x_i)\| =$
1003 1, the Euclidean distance between $f_\phi(x_i)$ and $f_\phi(x_j)$ is $2 - 2(f_\phi(x_i) \cdot f_\phi(x_j))$.

1004 The InfoNCE loss can be written in its standard form:

$$1007 \mathcal{L}_{\text{InfoNCE}} = - \sum_i \log \frac{\exp(f_\phi(x_i) \cdot f_\phi(x_i^+)/\tau)}{1008 \sum_k \exp(f_\phi(x_i) \cdot f_\phi(x_k)/\tau)},$$

1009 where j^+ is the index of a positive pair for i . Alternatively, in terms of cross-entropy, the loss
1010 becomes:

$$1012 \mathcal{L}_{\text{InfoNCE}} \propto \sum_i \sum_j p_\theta(j|i) \log q_\phi(j|i) = H(p_\theta, q_\phi),$$

1013 where $H(p_\theta, q_\phi)$ denotes the cross-entropy between the two distributions. Since $p_\theta(j|i)$ is
1014 fixed, minimizing the cross-entropy $H(p_\theta, q_\phi)$ is equivalent to minimizing the KL divergence
1015 $D_{\text{KL}}(p_\theta \| q_\phi)$. By aligning the learned distribution $q_\phi(j|i)$ with the target distribution $p_\theta(j|i)$,
1016 InfoNCE operates within the I-Con framework, where the neighborhood structure in the original space
1017 is preserved in the embedding space. Thus, InfoNCE is a direct instance of I-Con, optimizing the
1018 same divergence-based objective. \square

1019
1020 **Corollary 2.** *The Supervised Contrastive Loss Khosla et al. (2020) is an instance of the I-Con
1021 framework.*

1022
1023 *Proof.* This follows directly from Theorem 4. Define the supervisory and target distributions as:

$$1025 q_\phi(j | i) = \frac{\exp(f_\phi(x_i) \cdot f_\phi(x_j)/\tau)}{\sum_{k \neq i} \exp(f_\phi(x_i) \cdot f_\phi(x_k)/\tau)},$$

$$p_\theta(j | i) = \frac{1}{K_i - 1} \mathbf{1}[i \text{ and } j \text{ share the same label}],$$

where f_ϕ is the mapping to deep feature space and K_i is the number of samples in the class of i . Substituting these definitions into the I-Con framework recovers the Supervised Contrastive Loss.

□

Theorem 5 (Triplet Loss Schroff et al. (2015)). *Triplet Loss can be viewed as an instance of the I-Con framework with the following distributions $p_\theta(j|i)$ and $q_\phi(j|i)$:*

$$p_\theta(j|i) = \begin{cases} \frac{1}{k} & \text{if } x_j \text{ is among the } k \text{ positive views of } x_i, \\ 0 & \text{otherwise,} \end{cases}$$

$$q_\phi(j|i) = \frac{\exp\left(-\frac{\|f_\phi(x_i) - f_\phi(x_j)\|^2}{\sigma^2}\right)}{\sum_{k \neq i} \exp\left(-\frac{\|f_\phi(x_i) - f_\phi(x_k)\|^2}{\sigma^2}\right)},$$

particularly in the special case where only two neighbors are considered: one positive view and one negative view.

Proof. The idea of this proof was first presented at Khosla et al. (2020) using Taylor Approximation; however, in this proof we present a stronger bounds for this result. For simplicity, we set $\sigma = 1$ (the general bounds for other σ values are provided at the end of the proof).

$$\mathcal{L} = -\frac{1}{N} \sum_i \sum_j q_\phi(j|i) \log \frac{\exp(-\|f_\phi(x_i) - f_\phi(x_j)\|^2)}{\sum_{k \neq i} \exp(-\|f_\phi(x_i) - f_\phi(x_k)\|^2)}.$$

In the special case where each anchor x_i has exactly one positive x_i^+ and one negative x_i^- example, the denominator simplifies to:

$$\sum_{k \neq i} \exp(-\|f_\phi(x_i) - f_\phi(x_k)\|^2) = \exp(-\|f_\phi(x_i) - f_\phi(x_i^+)\|^2) + \exp(-\|f_\phi(x_i) - f_\phi(x_i^-)\|^2).$$

Let $d_i^+ = \|f_\phi(x_i) - f_\phi(x_i^+)\|^2$ and $d_i^- = \|f_\phi(x_i) - f_\phi(x_i^-)\|^2$. Substituting these into the loss function, we obtain:

$$\begin{aligned} \mathcal{L} &= -\frac{1}{N} \sum_i \log \frac{\exp(-d_i^+)}{\exp(-d_i^+) + \exp(-d_i^-)} \\ &= -\frac{1}{N} \sum_i \log \left(\frac{1}{1 + \exp(d_i^- - d_i^+)} \right) \\ &= \frac{1}{N} \sum_i \log(1 + \exp(d_i^+ - d_i^-)). \end{aligned}$$

Recognizing that the expression inside the logarithm is the softplus function, we can leverage its well-known bounds:

$$\max(z, 0) \leq \log(1 + \exp(z)) \leq \max(z, 0) + \log(2).$$

By letting $z = d_i^+ - d_i^-$, we substitute into the bounds to obtain:

$$\frac{1}{N} \sum_i \max(d_i^+ - d_i^-, 0) \leq \mathcal{L} \leq \frac{1}{N} \sum_i \max(d_i^+ - d_i^-, 0) + \log(2),$$

where the left-hand side is the Triplet loss $\mathcal{L}_{\text{Triplet}} = \frac{1}{N} \sum_i \max(d_i^+ - d_i^-, 0)$. Therefore, we obtain the following bounds:

$$\mathcal{L} - \log(2) \leq \mathcal{L}_{\text{Triplet}} \leq \mathcal{L}.$$

For a general σ , the inequality bounds are as follows:

$$\mathcal{L}_\sigma - \sigma^2 \log(2) \leq \mathcal{L}_{\text{Triplet}} \leq \mathcal{L}_\sigma,$$

1080 where

$$1081 \quad \mathcal{L}_\sigma = -\frac{\sigma^2}{N} \sum_i \sum_j q_\phi(j|i) \log \frac{\exp\left(-\frac{\|f_\phi(x_i) - f_\phi(x_j)\|^2}{\sigma^2}\right)}{\sum_{k \neq i} \exp\left(-\frac{\|f_\phi(x_i) - f_\phi(x_k)\|^2}{\sigma^2}\right)}.$$

1085 As σ approaches 0, $\mathcal{L}_{\text{Triplet}}$ approaches \mathcal{L}_σ . \square

1086 **Theorem 6.** *Contrastive Multiview Coding (CMC) and CLIP are instances of the I-Con framework.*

1089 *Proof.* Since we have already established that InfoNCE is an instance of the I-Con framework, this
1090 corollary follows naturally. The key difference in Contrastive Multiview Coding (CMC) and CLIP is
1091 that they optimize alignment across different modalities. The target probability distribution $p_\theta(j|i)$
1092 can be expressed as:

$$1093 \quad p_\theta(j|i) = \frac{1}{Z} \mathbb{1}[i \text{ and } j \text{ are positive pairs and } V_i \neq V_j],$$

1095 where V_i and V_j represent the modality sets of x_i and x_j , respectively. Here, $p_\theta(j|i)$ assigns uniform
1096 probability over positive pairs drawn from different modalities.

1098 The learned distribution $q_\phi(j|i)$, in this case, is based on a Gaussian similarity between deep fea-
1099 tures, but conditioned on points from the opposite modality set. Thus, the learned distribution is
1100 defined as:

$$1101 \quad q_\phi(j|i) = \frac{\exp(-\|f_\phi(x_i) - f_\phi(x_j)\|^2)}{\sum_{k \in V_j} \exp(-\|f_\phi(x_i) - f_\phi(x_k)\|^2)}.$$

1104 This formulation shows that CMC and CLIP follow the same principles as InfoNCE but apply them
1105 in a multiview setting, fitting seamlessly within the I-Con framework by minimizing the divergence
1106 between the target and learned distributions across different modalities. \square

1107 **Corollary 3.** *Cross-Entropy classification is an instance of the I-Con framework.*

1109 *Proof.* Cross-Entropy can be viewed as a special case of the CMC loss, where one "view" corre-
1110 sponds to the data point features and the other to the class logits. The affinity between a data point
1111 and a class is based on whether the point belongs to that class. This interpretation has been explored
1112 in prior work, where Cross-Entropy was shown to be related to the CLIP loss Yang et al. (2022). \square

1114 **Theorem 7.** *Masked Language Modeling (MLM) Devlin et al. (2019) loss is an instance of the
1115 I-Con framework.*

1117 *Proof.* In Masked Language Modeling, the objective is to predict a masked token j given its sur-
1118 rounding context x_i . This setup fits naturally within the I-Con framework by defining appropriate
1119 target and learned distributions.

1121 The target distribution $p_\theta(j|i)$ is the empirical distribution over contexts i and tokens j , defined as:

$$1122 \quad p_\theta(j|i) = \frac{1}{Z} \# [\text{Context } i \text{ precedes token } j],$$

1125 where $\# [\text{Context } i \text{ precedes token } j]$ counts the number of times token j follows context x_i in the
1126 training corpus and Z is a normalization constant ensuring that $\sum_j p_\theta(j|i) = 1$.

1127 The learned distribution $q_\phi(j|i)$ is modeled using the neural network's output logits for token pre-
1128 dictions. It is defined as a softmax over the dot product between the context embedding $f_\phi(x_i)$ and
1129 the token embeddings ϕ_j :

$$1130 \quad q_\phi(j|i) = \frac{\exp(f_\phi(x_i) \cdot \phi_j)}{\sum_{k \in \mathcal{V}} \exp(f_\phi(x_i) \cdot \phi_k)},$$

1133 where $f_\phi(x_i)$ is the embedding of the context x_i produced by the model, ϕ_j is the embedding of
token j , and \mathcal{V} is the vocabulary of all possible tokens.

1134 The MLM loss aims to minimize the cross-entropy between the target distribution $p_\theta(j|i)$ and the
 1135 learned distribution $q_\phi(j|i)$:
 1136

$$1137 \quad \mathcal{L}_{\text{MLM}} = - \sum_i \sum_j p_\theta(j|i) \log q_\phi(j|i) = H(p_\theta, q_\phi).$$

1139 Since in practice, for each context x_i , only the true masked token j_i^* is considered, the target distribution
 1140 simplifies to:
 1141

$$1142 \quad p_\theta(j|i) = \delta_{j,j_i^*},$$

1143 where δ_{j,j_i^*} is the Kronecker delta function, equal to 1 if $j = j_i^*$ and 0 otherwise.
 1144

Substituting this into the loss function, the MLM loss becomes:
 1145

$$1146 \quad \mathcal{L}_{\text{MLM}} = - \sum_i \log q_\phi(j_i^*|x_i).$$

□

D UNIFYING CLUSTERING METHODS

The connections between clustering and the I-Con framework are more intricate compared to the dimensionality reduction methods discussed earlier. To establish these links, we first introduce a probabilistic formulation of K-means and demonstrate its equivalence to the classical K-means algorithm, showing that it is a zero-gap relaxation. Building upon this, we reveal how probabilistic K-means can be viewed as an instance of I-Con, leading to a novel clustering kernel. Finally, we show that several clustering methods implicitly approximate and optimize for this kernel.

Definition 1 (Classical K-means). *Let $x_1, x_2, \dots, x_N \in \mathbb{R}^n$ denote the data points, and $\mu_1, \mu_2, \dots, \mu_m \in \mathbb{R}^n$ be the cluster centers.*

The objective of classical K-means is to minimize the following loss function:

$$1162 \quad \mathcal{L}_{\text{k-Means}} = \sum_{i=1}^N \sum_{c=1}^m \mathbb{1}(c^{(i)} = c) \|x_i - \mu_c\|^2,$$

where $c^{(i)}$ represents the cluster assignment for data point x_i , and is defined as:

$$1167 \quad c^{(i)} = \arg \min_c \|x_i - \mu_c\|^2.$$

D.1 PROBABILISTIC K-MEANS RELAXATION

In probabilistic K-means, the cluster assignments are relaxed by assuming that each data point x_i belongs to a cluster c with probability ϕ_{ic} . In other words, ϕ_i represents the cluster assignments vector for x_i

Proposition 2. *The relaxed loss function for probabilistic K-means is given by:*

$$1176 \quad \mathcal{L}_{\text{Prob-k-Means}} = \sum_{i=1}^N \sum_{c=1}^m \phi_{ic} \|x_i - \mu_c\|^2,$$

and is equivalent to the original K-means objective $\mathcal{L}_{\text{k-Means}}$. The optimal assignment probabilities ϕ_{ic} are deterministic, assigning probability 1 to the closest cluster and 0 to others.

Proof. For each data point x_i , the term $\sum_{c=1}^m \phi_{ic} \|x_i - \mu_c\|^2$ is minimized when the assignment probabilities ϕ_{ic} are deterministic, i.e.,

$$1184 \quad \phi_{ic} = \begin{cases} 1 & \text{if } c = \arg \min_j \|x_i - \mu_j\|^2, \\ 0 & \text{otherwise.} \end{cases}$$

With these deterministic probabilities, $\mathcal{L}_{\text{Prob-k-Means}}$ simplifies to the classical K-means objective, confirming that the relaxation introduces no gap. □

1188 D.1.1 CONTRASTIVE FORMULATION OF PROBABILISTIC K-MEANS
11891190 **Definition 2.** Let $\{x_i\}_{i=1}^N$ be a set of data points. Define the conditional probability $q_\phi(j|i)$ as:
1191

1192
$$q_\phi(j|i) = \sum_{c=1}^m \frac{\phi_{ic}\phi_{jc}}{\sum_{k=1}^N \phi_{kc}},$$

1193

1194 where ϕ_i is the soft-cluster assignments for x_i .
11951196 Given $q_\phi(j|i)$, we can reformulate probabilistic K-means as a contrastive loss:
11971198 **Theorem 8.** Let $\{x_i\}_{i=1}^N \in \mathbb{R}^n$ and $\{\phi_{ic}\}_{i=1}^N$ be the corresponding assignment probabilities. Define
1199 the objective function \mathcal{L} as:
1200

1201
$$\mathcal{L} = - \sum_{i,j} (x_i \cdot x_j) q_\phi(j|i).$$

1202 Minimizing \mathcal{L} with respect to the assignment probabilities $\{\phi_{ic}\}$ yields optimal cluster assignments
1203 equivalent to those obtained by K-means.
12041205 *Proof.* The relaxed probabilistic K-means objective $\mathcal{L}_{\text{Prob-k-Means}}$ is:
1206

1207
$$\mathcal{L}_{\text{Prob-k-Means}} = \sum_{i=1}^N \sum_{c=1}^m \phi_{ic} \|x_i - \mu_c\|^2.$$

1208

1209 Expanding this, we obtain:
1210

1211
$$\mathcal{L}_{\text{Prob-k-Means}} = \sum_{c=1}^m \left(\sum_{i=1}^N \phi_{ic} \right) \|\mu_c\|^2 - 2 \sum_{c=1}^m \left(\sum_{i=1}^N \phi_{ic} x_i \right) \cdot \mu_c + \sum_{i=1}^N \|x_i\|^2.$$

1212

1213 The cluster centers μ_c that minimize this loss are given by:
1214

1215
$$\mu_c = \frac{\sum_{i=1}^N \phi_{ic} x_i}{\sum_{i=1}^N \phi_{ic}}.$$

1216

1217 Substituting μ_c back into the loss function, we get:
1218

1219
$$\mathcal{L} = - \sum_{i,j} (x_i \cdot x_j) q_\phi(j|i),$$

1220

1221 which proves that minimizing this contrastive formulation leads to the same clustering assignments
1222 as classical K-means. \square
12231224 **Corollary 4.** The alternative loss function:
1225

1226
$$\mathcal{L} = - \sum_{i,j} \|x_i - x_j\|^2 q_\phi(j|i),$$

1227

1228 yields the same optimal clustering assignments when minimized with respect to $\{\phi_{ic}\}$.
12291230 *Proof.* Expanding the squared norm in the loss function gives:
1231

1232
$$\mathcal{L} = - \sum_{i,j} (\|x_i\|^2 - 2x_i \cdot x_j + \|x_j\|^2) q_\phi(j|i).$$

1233

1234 The terms involving $\|x_i\|^2$ and $\|x_j\|^2$ simplify since $\sum_j q_\phi(j|i) = 1$, reducing the loss to:
1235

1236
$$\mathcal{L} = 2 \left(- \sum_{i,j} x_i \cdot x_j q_\phi(j|i) \right),$$

1237

1238 which is equivalent to the objective in the previous theorem. \square
1239

1242 D.2 PROBABILISTIC K-MEANS AS AN I-CON METHOD
 1243

1244 In the I-Con framework, the target and learned distributions represent affinities between data points
 1245 based on specific measures. For instance, in SNE, these measures are Euclidean distances in high-
 1246 and low-dimensional spaces, while in SupCon, the distances reflect whether data points belong to
 1247 the same class. Similarly, we can define a measure of neighborhood probabilities in the context
 1248 of clustering, where two points are considered neighbors if they belong to the same cluster. The
 1249 probability of selecting x_j as x_i 's neighbor is the probability that a point, chosen uniformly at
 1250 random from x_i 's cluster, is x_j . More explicitly, let $q_\phi(j|i)$ represent the probability that x_j is
 1251 selected uniformly at random from x_i 's cluster:

1252
$$q_\phi(j|i) = \sum_{c=1}^m \frac{\phi_{ic}\phi_{jc}}{\sum_{k=1}^N \phi_{kc}}.$$

 1253
 1254

1255 **Theorem 9** (K-means as an instance of I-Con). *Given data points $\{x_i\}_{i=1}^N$, define the neighborhood
 1256 probabilities $p_\theta(j|i)$ and $q_\phi(j|i)$ as:*

1257
$$p_\theta(j|i) = \frac{\exp(-\|x_i - x_j\|^2/2\sigma^2)}{\sum_k \exp(-\|x_i - x_k\|^2/2\sigma^2)}, \quad q_\phi(j|i) = \sum_{c=1}^m \frac{\phi_{ic}\phi_{jc}}{\sum_{k=1}^N \phi_{kc}}.$$

 1258
 1259

1260 Let the loss function \mathcal{L}_{c-SNE} be the sum of KL divergences between the distributions $q_\phi(j|i)$ and
 1261 $p_\theta(j|i)$:

1262
$$\mathcal{L}_{c-SNE} = \sum_i D_{KL}(q_\phi(\cdot|i) \| p_\theta(\cdot|i)).$$

 1263
 1264

1265 Then,

1266
$$\mathcal{L}_{c-SNE} = \frac{1}{2\sigma^2} \mathcal{L}_{Prob-k-Means} - \sum_i H(q_\phi(\cdot|i)),$$

 1267

1268 where $H(q_\phi(\cdot|i))$ is the entropy of $q_\phi(\cdot|i)$.

1269 *Proof.* For simplicity, assume that $2\sigma^2 = 1$. Denote $\sum_k \exp(-\|x_i - x_k\|^2)$ by Z_i . Then we have:

1270
$$\log p_\theta(j|i) = -\|x_i - x_j\|^2 - \log Z_i.$$

 1271
 1272

1273 Let \mathcal{L}_i be defined as $-\sum_j \|x_i - x_j\|^2 q_\phi(j|i)$. Using the equation above, \mathcal{L}_i can be rewritten as:

1274
$$\mathcal{L}_i = -\sum_j \|x_i - x_j\|^2 q_\phi(j|i) \tag{3}$$

 1275
 1276

1277
$$= \sum_j (\log(p_\theta(j|i)) + \log(Z_i)) q_\phi(j|i) \tag{4}$$

 1278
 1279

1280
$$= \sum_j q_\phi(j|i) \log(p_\theta(j|i)) + \sum_j q_\phi(j|i) \log(Z_i) \tag{5}$$

 1281
 1282

1283
$$= \sum_j q_\phi(j|i) \log(p_\theta(j|i)) + \log(Z_i) \tag{6}$$

 1284
 1285

1286
$$= H(q_\phi(\cdot|i), p_\theta(\cdot|i)) + \log(Z_i) \tag{7}$$

 1287

1288
$$= D_{KL}(q_\phi(\cdot|i) \| p_\theta(\cdot|i)) + H(q_\phi(\cdot|i)) + \log(Z_i). \tag{8}$$

1289 Therefore, $\mathcal{L}_{Prob-KMeans}$, as defined in Corollary 4, can be rewritten as:

1290
$$\mathcal{L}_{Prob-KMeans} = -\sum_i \sum_j \|x_i - x_j\|^2 q_\phi(j|i) = \sum_i \mathcal{L}_i \tag{9}$$

 1291
 1292

1293
$$= \sum_i D_{KL}(q_\phi(\cdot|i) \| p_\theta(\cdot|i)) + H(q_\phi(\cdot|i)) + \log(Z_i) \tag{10}$$

 1294
 1295

1296
$$= \mathcal{L}_{c-SNE} + \sum_i H(q_\phi(\cdot|i)) + \text{constant}. \tag{11}$$

1296 Therefore,

$$\mathcal{L}_{\text{c-SNE}} = \mathcal{L}_{\text{Prob-KMeans}} - \sum_i H(q_\phi(\cdot|i)).$$

1297 If we allow σ to take any value, the entropy penalty will be weighted accordingly:

$$\mathcal{L}_{\text{c-SNE}} = \frac{1}{2\sigma^2} \mathcal{L}_{\text{Prob-KMeans}} - \sum_i H(q_\phi(\cdot|i)).$$

1298 Note that the relation above is up to an additive constant. This implies that minimizing the contrastive probabilistic K-means loss with entropy regularization minimizes the sum of KL divergences between $q_\phi(\cdot|i)$ and $p_\theta(\cdot|i)$. \square

1300 **Theorem 10.** *Mutual Information Clustering is an instance of I-Con.*

1301 *Proof.* Given the connection established between SimCLR, K-Means, and the I-Con framework, this result follows naturally. Specifically, the target distribution $p_\theta(j|i)$ (the supervised part) is a uniform distribution over observed positive pairs:

$$p_\theta(j|i) = \begin{cases} \frac{1}{k} & \text{if } x_j \text{ is among the } k \text{ positive views of } x_i, \\ 0 & \text{otherwise.} \end{cases}$$

1302 On the other hand, the learned embeddings ϕ_i represent the probabilistic assignments of x_i into clusters. Therefore, similar to the analysis of the K-Means connection, the learned distribution is modeled as:

$$q_\phi(j|i) = \sum_{c=1}^m \frac{\phi_{ic}\phi_{jc}}{\sum_{k=1}^N \phi_{kc}}.$$

1303 This shows that Mutual Information Clustering can be viewed as a method within the I-Con framework, where the learned distribution $q_\phi(j|i)$ aligns with the target distribution $p_\theta(j|i)$, completing the proof. \square

1304 **Corollary 5.** *Spectral Clustering is an instance of the I-Con framework.*

1305 *Proof.* From Theorem 9, we know that K-Means clustering can be formulated as an instance of the I-Con framework, where the clustering assignments depend on the inner products of the data points.

1306 Spectral Clustering extends this idea by first embedding the data into a lower-dimensional space using the top k eigenvectors of the normalized Laplacian derived from the affinity matrix A . The affinity matrix A is constructed using a similarity measure (e.g., an RBF kernel) and encodes the probabilities of assignments between data points. Given this transformation, spectral clustering is an instance of I-Con on the projected embeddings. \square

1307 **Theorem 11.** *Normalized Cuts Shi & Malik (2000) is an instance of I-Con.*

1308 *Proof.* The proof for this follows naturally from our work on K-Means analysis. The loss function for normalized cuts is defined as:

$$\mathcal{L}_{\text{NormCuts}} = \sum_{c=1}^m \frac{\text{cut}(A_c, \bar{A}_c)}{\text{vol}(A_c)},$$

1309 where A_c is a subset of the data corresponding to cluster c , \bar{A}_c is its complement, and $\text{cut}(A_c, \bar{A}_c)$ represents the sum of edge weights between A_c and \bar{A}_c , while $\text{vol}(A_c)$ is the total volume of cluster A_c , i.e., the sum of edge weights within A_c .

1310 Similar to K-Means, by reformulating this in a contrastive style with soft-assignments, the learned distribution can be expressed using the probabilistic cluster assignments $\phi_{ic} = p(c|x_i)$ as:

$$q_\phi(j|i) = \sum_{c=1}^m \frac{\phi_{ic}\phi_{jc}d_j}{\sum_{k=1}^N \phi_{kc}d_k},$$

1311 where d_j is the degree of node x_j , and the volume and cut terms can be viewed as weighted sums over the soft-assignments of data points to clusters.

This reformulation shows that normalized cuts can be written in a manner consistent with the I-Con framework, where the target distribution $p_\theta(j|i)$ and the learned distribution $q_\phi(j|i)$ represent affinity relationships based on graph structure and cluster assignments.

Thus, normalized cuts is an instance of I-Con, where the loss function optimizes the neighborhood structure based on the cut and volume of clusters in a manner similar to K-Means and its probabilistic relaxations. \square

E I-CON AS A VARIATIONAL METHOD

Variational bounds for mutual information are widely explored and have been connected to loss functions such as InfoNCE, where minimizing InfoNCE maximizes the mutual information lower bound Oord et al. (2018); Poole et al. (2019). The proof usually starts by rewriting the mutual information:

$$I(X; Y) = \mathbb{E}_{p(x,y)} \left[\log \frac{q(x|y)}{p(x)} \right] + \mathbb{E}_{p(y)} [D_{\text{KL}}(p(x|y) \| q(x|y))]$$

This expression is typically used to derive a lower bound for $I(X; Y)$. The proof usually begins by assuming that p is uniform over discrete data points $\mathcal{X} = \{x_i\}_{i=1}^N$ (i.e., we use uniform sampling for data points). By using the fact that $p(x_i) = \frac{1}{N}$, we can write $p(x, y) = \frac{1}{N}p(x|y)$. Therefore, the mutual information lower bound becomes

$$\begin{aligned} I(X; Y) &\geq \mathbb{E}_{p(x,y)} [\log q(x|y)] - \mathbb{E}_{p(x,y)} [\log p(x)] \\ &= \mathbb{E}_{p(x,y)} [\log q(x|y)] + \log(N) \\ &= \frac{1}{N} \sum_{x,y \in \mathcal{X} \times \mathcal{X}} p(x|y) \log q(x|y) + \log(N) \\ &= \frac{1}{N} \sum_{y \in \mathcal{Y}} \sum_{x \in \mathcal{X}} p(x|y) \log q(x|y) + \log(N) \\ &= -H(p(x|y), q(x|y)) + \log(N) \end{aligned}$$

Therefore, maximizing the cross-entropy between the two distributions maximizes the mutual information between samples.

On the hand, Variational Bayesian (VB) methods are fundamental in approximating intractable posterior distributions $p(z | x)$ with tractable variational distributions $q_\phi(z)$. This approximation is achieved by minimizing the Kullback-Leibler (KL) divergence between the variational distribution and the true posterior:

$$\text{KL}(q_\phi(z) \| p(z | x)) = \mathbb{E}_{q_\phi(z)} \left[\log \frac{q_\phi(z)}{p(z | x)} \right]. \quad (12)$$

The optimization objective, known as the Evidence Lower Bound (ELBO), is given by:

$$\text{ELBO} = \mathbb{E}_{q_\phi(z)} [\log p(x, z)] - \mathbb{E}_{q_\phi(z)} [\log q_\phi(z)]. \quad (13)$$

Maximizing the ELBO is equivalent to minimizing the KL divergence, thereby ensuring that $q_\phi(z)$ closely approximates $p(z | x)$ Blei et al. (2017).

VB can be framed within the I-Con framework by making specific mappings between the variables and distributions. Let i correspond to the data point x , and j correspond to the latent variable z . We can set the supervisory distribution $p_\theta(z | x)$ to be the true posterior $p(z | x)$. This allow us to define the learned distribution $q_\phi(z | x)$ to be independent of x , i.e., $q_\phi(z | x) = q_\phi(z)$.

Under these settings, the I-Con loss simplifies to:

$$\mathcal{L}(\phi) = \int_{x \in \mathcal{X}} \text{KL}(p(z | x) \| q_\phi(z)) dx = \mathbb{E}_{p(x)} [\text{KL}(p(z | x) \| q_\phi(z))]. \quad (14)$$

1404 E.1 INTERPRETATION
1405

- Global Approximation: In VB, $q_\phi(z)$ serves as a global approximation to the posterior $p(z | x)$ across all data points x . Similarly, in I-Con, when $q_\phi(j | i) = q_\phi(j)$, the learned distribution provides a uniform approximation across all i .
- Variational Alignment: Both frameworks employ variational techniques to align a tractable distribution q_ϕ with an intractable or supervisory distribution p . This alignment ensures that the learned representations capture essential information from the target distribution.
- Framework Generalization: I-Con generalizes VB by allowing $q_\phi(j | i)$ to depend on i , enabling more flexible and data-specific alignments. VB is recovered as a special case where the learned distribution is uniform across all data points.

1416 F WHY DO WE NEED TO UNIFY REPRESENTATION LEARNERS?
1417

I-con not only provides a deeper understanding of these methods but also opens up the possibility of creating new methods by mixing and matching components. We explicitly use this property to discover new improvements to both clustering and representation learners. In short, I-Con acts like a periodic table of machine learning losses. With this periodic table we can more clearly see the implicit assumptions of each method by breaking down modern ML losses into more simple components: pairwise conditional distributions p and q .

One particular example of how this opens new possibilities is with our generalized debiasing operation. Through our experiments we show adding a slight constant linkage between datapoints improves both stability and performance across clustering and feature learning. Unlike prior art, which only applies to specific feature learners, our debiasers can improve clusterers, feature learners, spectral graph methods, and dimensionality reducers.

Finally it allows us to discover novel theoretical connections by compositionally exploring the space, and considering limiting conditions. We use I-Con to help derive a novel theoretical equivalences between K-Means and contrastive learning, and between MDS, PCA, and SNE. Transferring ideas between methods is standard in research, but in our view it becomes much simpler to do this if you know methods are equivalent. Previously, it might not be clear how exactly to translate an insight like changing Gaussian distributions to Cauchy distributions in the upgrade from SNE to T-SNE has any effect on clustering or representation learning. In I-Con it becomes clear to see that similarly softening clustering and representation learning distributions can improve performance and debias representations.

1439 G HOW TO CHOOSE NEIGHBORHOOD DISTRIBUTIONS FOR YOUR PROBLEM
14401441 G.1 PARAMETERIZATION OF LEARNING SIGNAL
1442

- **Parametric:** (Learn a network to transform a data points to representations). Use a parametric method to quickly represent new datapoints without retraining. Use a parametric method if there is enough “features” in the underlying data to properly learn a representation. Use this option with datasets with sparse supervisory signal in order to share learning signal through network parameters.
- **Nonparametric:** (Learn one representation per data point). Use a nonparametric method if datapoints are abstract and don’t contain natural features that are useful for mapping. Use this option to better optimize the loss of each individual datapoint. Do not use this in sparse supervisory signal regimes (Like augmentation based contrastive learning), as there are not enough links to resolve each individual embedding.

1453 G.2 CHOICE OF SUPERVISORY SIGNAL
1454

- **Gaussians on distances in the input space:** though this is a common choice and underlies methods like k-means, with enough data it is almost always better to use k-neighbor distributions as they better capture local topology of data. This is the same intuition that is used to justify spectral clustering over k-means.

- **K-neighbor graphs distributions:** If your data can be naturally put into a graph instead of just considering Gaussians on the input space we suggest it. This allows the algorithm to adapt local neighborhoods to the data, as opposed to considering all points neighborhoods equally shaped and sized. This better aligns with the manifold hypothesis.
- **Contrastive augmentations:** When possible, add contrastive augmentations to your graph - this will improve performance in cases where quantities of interest (like an image class) are guaranteed to be shared between augmentations.
- **General kernel smoothing techniques:** Use random walks to improve the optimization quality. It connects more points together and in some cases mirrors geodesic distance on the manifold Crane et al. (2013).
- **Debiasing:** Use this if you think negative pairs actually have a small chance of aligning positively. For a small number of classes this parameter scales like the inverse of the number of classes. You can also use this to improve stability of the optimization.

G.3 CHOICE OF REPRESENTATION:

Any conditional distribution on representations can be used, so consider what kind of structure you want to learn, tree, vector, cluster, etc. And choose the distribution to be simple and meaningful for that representation.

- **Discrete:** Use discrete cluster-based representations if interpretability and discrete structure are important
- **Continuous Vector:** Use a vector representation if generic downstream performance is a concern as this is a bit easier to optimize than discrete variants.

H COMPARING I-CON, MLE, AND THE KL DIVERGENCE

There are many connections between KL divergence and maximum likelihood estimation. We highlight the differences between a standard MLE approach and I-Con. In short, although I-Con has a maximum likelihood interpretation, its specific functional form allows it to unify both unsupervised and supervised methods in a way that elucidates the key structures that are important for deriving new representation learning losses. This is in contrast to the commonly known connection between MLE and KL divergence minimization, which does not focus on pairwise connections between datapoints and does not provide as much insight for representation learners. To see this we note that the conventional connection between MLE and KL minimization is as follows:

$$\theta_{\text{MLE}} = \arg \min_{\theta} D_{\text{KL}}(\hat{P} || Q_{\theta}),$$

where the empirical distribution, \hat{P} , is defined as:

$$\hat{P}(x) = \frac{1}{N} \sum_{i=1}^N \delta(x - x_i),$$

where $\delta(x - x_i)$ is the Dirac delta function. The classical KL minimization fits a parameterized model family to an empirical distribution. In contrast the I-Con equation:

$$\mathcal{L}(\theta, \phi) = \int_{i \in \mathcal{X}} D_{\text{KL}}(p_{\theta}(\cdot | i) || q_{\phi}(\cdot | i))$$

Operates on conditional distributions and captures an “average” KL divergence instead of a single KL divergence. Secondly, I-Con explicitly involves a computation over neighboring datapoints which does not appear in the aforementioned equation. This decomposition of methods into their actions on their neighborhoods makes many methods simpler to understand, and makes modifications of these methods easier to transfer between domains. It also makes it possible to apply this theory to unsupervised problems where empirical supervisory data does not exist. Furthermore some methods, like DINO, do not share the exact functional form of I-Con, and suffer from various difficulties

1512 like collapse which need to be handled with specific regularizers. This shows that I-Con is not just a
1513 catchall reformulation of MLE, but is capturing a specific functional form shared by several popular
1514 learners.
1515

1516 I ON I-CON’S HYPERPARAMETERS 1517

1518 One important way that I-Con removes hyperparameters from existing works is that it does not rely
1519 on things like entropy penalties, activation normalization, activation sharpening, or EMA stabilization
1520 to avoid collapse. The loss is self-balancing in this regard as any way that it can improve the
1521 learned distribution to better match the target distribution is “fair game”. This allows one to general-
1522 ize certain aspects of existing losses like InfoNCE. In I-Con info NCE looks like fixed-width
1523 Gaussian kernels mediating similarity between representation vectors. In I-Con it’s trivial to gener-
1524 alize these Gaussians to have adaptive and learned covariances for example. This allows the network
1525 to select its own level of certainty in representation learning. If you did this naively, you would need
1526 to ensure the loss function doesn’t cheat by making everything less certain.

1527 Nevertheless I-Con defines a space of methods depending on the choice of p and q. The choice of
1528 these two distributions becomes the main source of hyperparameters we explore. In particular our
1529 experiments change the structure of the supervisory signal (often p). For example, in a clustering
1530 experiment changing p from “Gaussians with respect to distance” to “graph adjacency” transforms
1531 K-Means into Spectral clustering. It’s important to note that K-means has benefits over Spectral
1532 clustering in certain circumstances and vice-versa, and there’s not necessarily a singular “right”
1533 choice for p in every problem. Like many things in ML, the different supervisory distributions
1534 provide different inductive biases and should be chosen thoughtfully. We find that this design space
1535 makes it easier to build better performing supervisory signals for specific important problems like
1536 unsupervised image classification on ImageNet and others.
1537
1538
1539
1540
1541
1542
1543
1544
1545
1546
1547
1548
1549
1550
1551
1552
1553
1554
1555
1556
1557
1558
1559
1560
1561
1562
1563
1564
1565